

State-dependent errors in a land surface model across biomes inferred from eddy covariance observations on multiple timescales

Tao Wang^{a,*}, Pierre Brender^{b,a,**}, Philippe Ciais^a, Shilong Piao^c, Miguel D. Mahecha^d, Frédéric Chevallier^a, Markus Reichstein^d, Catherine Ottlé^a, Fabienne Maignan^a, Altaf Arain^e, Gil Bohrer^f, Alessandro Cescatti^g, Gerard Kiely^h, Beverly Elizabeth Lawⁱ, Merbold Lutz^j, Leonardo Montagnani^{k,l}, Eddy Moors^m, Bruce Osborneⁿ, Oleg Panferov^o, Dario Papale^p, Francesco Primo Vaccari^q

^a LSCE/IPSL, UMR8212, CEA-CNRS-UVSQ – Unité Mixte de Recherche, CE L'Orme des Merisiers, Gif-sur-Yvette 91191, France

^b AgroParisTech, ENGREF, 19 avenue du Maine, F-75015 Paris, France

^c Department of Ecology, College of Urban and Environmental Science, and Key Laboratory for Earth Surface Processes of the Ministry of Education, Peking University, Beijing 100871, China

^d Max Planck Institute for Biogeochemistry, P.O. Box 10 01 64, 07701 Jena, Germany

^e School of Geography and Earth Sciences, McMaster University, Hamilton, ON L8S 4K1, Canada

^f Department of Civil and Environmental Engineering, Duke University, NC 27708, USA

^g Climate Change Unit, Inst. for Environment and Sustainability, European Commission, DG Joint Research Centre, Ispra, Italy

^h HYDROMET, Civil and Environmental Engineering Dept., University College Cork, Ireland

ⁱ Department of Forest Ecosystems and Society, 328 Richardson Hall, Oregon State University, Corvallis, OR 97331, USA

^j ETH Zurich, Institute of Agricultural Sciences, Grassland Sciences Group, 8092 Zürich, Switzerland

^k Autonomous Province of Bolzano, Forest Services and Agency for the Environment, Bolzano, Italy

^l Free University of Bolzano, Faculty of Science and Technology, Bolzano, Italy

^m Alterra Green World Research, P.O. Box 47, Wageningen NL 6700 AA, The Netherlands

ⁿ University College Dublin, School of Biology and Environmental Science, Belfield, Dublin 4, Ireland

^o Department of Bioclimatology, University of Göttingen, Göttingen, Germany

^p Department for Innovation in Biological, Agro-food and Forest Systems (DIBAF), University of Tuscia, Italy

^q Institute of Biometeorology, National Research Council, Via Caproni, 8, 50145 Firenze, Italy

ARTICLE INFO

Article history:

Received 26 March 2012

Received in revised form 3 July 2012

Accepted 4 July 2012

Keywords:

Eddy covariance

Land surface model

State-dependent model bias

Neural networks

Singular system analysis

Timescale

ABSTRACT

Characterization of state-dependent model biases in land surface models can highlight model deficiencies, and provide new insights into model development. In this study, artificial neural networks (ANNs) are used to estimate the state-dependent biases of a land surface model (ORCHIDEE: ORGANISING Carbon and Hydrology in Dynamic Ecosystems). To characterize state-dependent biases in ORCHIDEE, we use multi-year flux measurements made at 125 eddy covariance sites that cover 7 different plant functional types (PFTs) and 5 climate groups. We determine whether the state-dependent model biases in five flux variables (H : sensible heat, LE : latent heat, NEE : net ecosystem exchange, GPP : gross primary productivity and R_{eco} : ecosystem respiration) are transferable within and between three different timescales (diurnal, seasonal–annual and interannual), and between sites (categorized by PFTs and climate groups). For each flux variable at each site, the spectral decomposition method (singular system analysis) was used to reconstruct time series on the three different timescales.

At the site level, we found that the share of state-dependent model biases (hereafter called “error transferability”) is larger for seasonal–annual and interannual timescales than for the diurnal timescale, but little error transferability was found between timescales in all flux variables. Thus, performing model evaluations at multiple timescales is essential for diagnostics and future development. For all PFTs, climate groups and timescale components, the state-dependent model biases are found to be transferable between sites within the same PFT and climate group, suggesting that specific model developments and improvements based on specific eddy covariance sites can be used to enhance the model performance at other sites within the same PFT-climate group. This also supports the legitimacy of upscaling from the

* Corresponding author. Tel.: +33 1 69 08 52 21; fax: +33 1 69 08 77 16.

** Corresponding author at: AgroParisTech, ENGREF, 19 avenue du Maine, F-75015 Paris, France. Tel.: +33 6 61 84 86 42; fax: +33 1 69 08 77 16.

E-mail addresses: tao.wang@lsce.ipsl.fr (T. Wang), pierre.brender@m4x.org (P. Brender).

ecosystem scale of eddy covariance sites to the regional scale based on the similarity of PFT and climate group. However, the transferability of state-dependent model biases between PFTs or climate groups is not always found on the seasonal–annual and interannual timescales, which is contrary to transferability found on the diurnal timescale and the original time series.

© 2012 Elsevier B.V. All rights reserved.

1. Introduction

The global eddy covariance network contains numerous on-line observations of CO₂, water, and energy fluxes across a range of biomes and timescales (Baldocchi et al., 2001; Baldocchi, 2008), with more than 965 site years in the La Thuile FLUXNET dataset (<http://www.fluxdata.org>). Recently, some large synthesis projects, such as the North American Carbon Program, have performed analysis over very large number of sites (e.g. Schaefer et al., 2012; Dietze et al., 2011; Richardson et al., 2012; Schwalm et al., 2010). Yet, many previous studies that quantified the performance of land surface models were based on much fewer sites (e.g. Thornton et al., 2002; Krinner et al., 2005) and assessed model performance with root mean square errors. Such characterization of model-observation mismatches do not distinguish between the random and the systematic parts of these errors. The model-observation mismatches result from several sources of errors. One is from structural deficiencies in the model representation of physical and biological processes and in the model initialization (Carvalhais et al., 2008), or in wrong values of model parameters. The others could be from model inputs as well as errors in eddy covariance measurements (Richardson et al., 2008; Lasslop et al., 2008; Abramowitz et al., 2007).

In order to characterize state-dependent model biases, recent studies (Dekker et al., 2001; Abramowitz, 2005; Abramowitz et al., 2007) demonstrated the value of explicitly quantifying state-dependent model biases as a function of chosen variables using artificial neural network (ANN) techniques. The idea is to establish a functional relationship between meteorological inputs (ANN inputs) and model-observation mismatch (ANN output) in a particular flux at a specific eddy covariance site by means of supervised training by ANN (the “ANN error model”). This error model is then applied to predict model-observation mismatches in an evaluation dataset not used for training. The state-dependent model bias could then be determined by quantifying the amount of the model-observation mismatch in the evaluation dataset that is accounted for by the error model. However, the state-dependent model biases could not always be fully documented since ANN inputs can be limited by both data availability and our current understanding of underlying processes. This methodology could potentially provide insights into the extent to which the state-dependent model bias is shared (hereafter transferable) between simulations of different environments, which may help to define directions for model improvements (Abramowitz et al., 2007). Abramowitz et al. (2007) examined the share of state-dependent model bias (hereafter called “transferability of state-dependent model bias”) across sites within and across vegetation types, and investigated the degree to which improvements of land surface models derived from a given site can be applied to other sites within the same vegetation type. They found that state-dependent model biases for both sensible and latent heat fluxes can be transferred within and across different vegetation types in the three models included in their study (CBM, CLM and a version of ORCHIDEE without dynamic vegetation). However, they did not investigate variations of the state-dependent model biases within a vegetation type that exists across different climate regimes or different timescales.

Previous studies (e.g. Siqueira et al., 2006; Mahecha et al., 2010a; Wang et al., 2011) reported model-observation mismatch

on different timescales in different ecosystem types, and pointed out that long timescales (e.g. seasonal–annual and interannual) always had larger relative model-observation mismatch than short timescales (e.g. diurnal). However, the systematic structure of model-observation mismatch in the timescale domain is still poorly understood. Equipped with the knowledge of transferability of state-dependent model bias within each timescale, modelers can make informed decisions on necessary developments. For example, one could prioritize new parameterizations to decrease state-dependent model biases for a specific purpose (e.g. a specific timescale). Furthermore, it is important to know whether improving a model for a process on a given timescale (e.g. diurnal variability of photosynthesis) also results in a better fit to observations on another timescale (e.g. seasonal or interannual variability of photosynthesis).

The aim of this study is to understand the extent to which state-dependent model biases are transferred in both space and timescale domains. To achieve this, a land surface model ORCHIDEE (ORganising Carbon and Hydrology in Dynamic Ecosystems) is used. ORCHIDEE is a Soil–Vegetation–Atmosphere–Transfer model, coupled to an ecosystem carbon model, that simulates energy, water and carbon exchanges between the atmosphere and the biosphere on different timescales, ranging from hours to centuries (Krinner et al., 2005). ORCHIDEE uses 12 plant functional types (PFTs) to describe vegetation distributions (Krinner et al., 2005). It can be run at both global and point scales, and a local point simulation forced by in situ meteorological data is performed in the present study. Point evaluation of ORCHIDEE simulations using eddy covariance datasets has been conducted on different timescales for all PFTs in previous studies (Krinner et al., 2005; Mahecha et al., 2010a). Here, we use a method of integrating time series decomposition into different timescales (singular system analysis: SSA, Mahecha et al., 2007, 2010a) and Artificial Neural Network (ANN, Chevallier et al., 1998) technique to quantify the error transferability in both space and timescale domains using 125 eddy covariance sites across the globe (obtained from the La Thuile FLUXNET database). The scientific questions addressed in this study are:

- (1) Are state-dependent model biases transferable within and across timescales?
- (2) Are state-dependent model biases transferable within and across PFTs and climate groups on different timescales?

2. Data and methods

2.1. Eddy covariance data

In this study, flux and meteorological drivers on half-hourly time steps are from Version 2 of the FLUXNET La Thuile dataset (<http://www.fluxdata.org>), and hourly time steps are aggregated from half-hourly data. We selected only sites with at least three years of data, and a data coverage of >70% within each year. A total of 125 sites are selected for the present study. For each site, climate is defined according to aggregated Köppen–Geiger classification (cf. <http://www.fluxdata.org>); vegetation class is from IGBP definitions, which is then classified to the corresponding PFT in ORCHIDEE. The distribution of studied sites with respect to PFT and climate groups

Table 1

The number of sites belonging to each PFT × climate group. Climate group is defined according to aggregated Köppen–Geiger classification.

Climate group/PFT	GRA	CRO	BoENF	TeENF	TeEBF	TeDBF	TrEBF
Boreal	2	0	18	0	0	1	0
Temperate	14	5	0	10	2	5	0
Temperate-continental	4	6	0	9	0	10	0
SubTropical-Mediterranean	5	4	0	9	4	9	0
Tropical	0	0	0	0	0	0	8

GRA: grassland; CRO: cropland; BoENF: boreal evergreen needleleaf forests; TeENF: temperate evergreen needleleaf forests; TeEBF: temperate evergreen broadleaf forests; TeDBF: temperate deciduous broadleaf forests; TrEBF: tropical evergreen broadleaf forests.

is displayed in Table 1, and their spatial distributions are shown in Fig. 1. In this study, shrublands and wetlands are not considered because ORCHIDEE do not have the corresponding PFT and related model parameterizations.

2.2. Simulation protocol

The ORCHIDEE model is driven with site meteorology. Our site selection criteria allow gaps in meteorological data (Section 2.1), so gap-filling algorithms (Appendix A) are applied to create continuous forcing data for model simulations.

The PFT for each site is prescribed in the model by using parameters that most closely represent the site vegetation and climate (Table B1). The soil and biomass carbon pools at each site are brought to the steady state by recycling the meteorological data. Site history in terms of management is not prescribed in the simulations.

2.3. Analysis methods

2.3.1. Singular system analysis (SSA)

Observed and modeled time series can be described as sets of subsignals, based on the assumption that these subsignals are dominated by characteristic scales of variability. Any time series is thus described as sets of additively superimposed subsignals

$$Y = \sum_{f=1}^F X_f \quad (1)$$

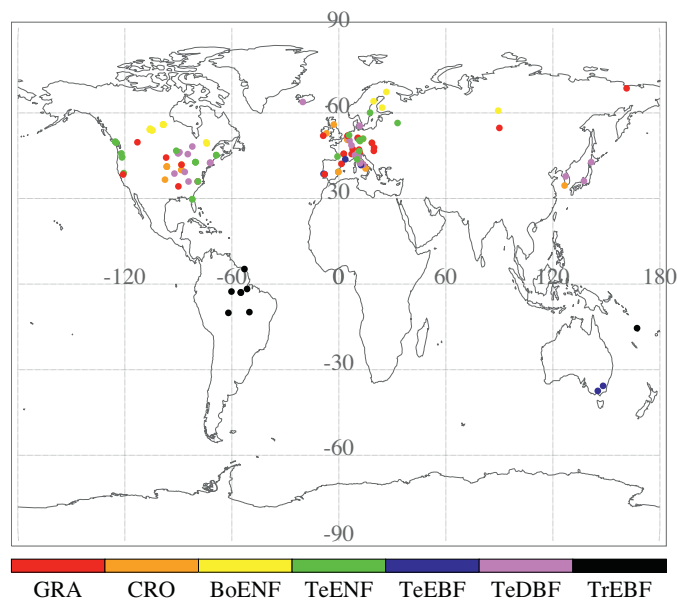


Fig. 1. Spatial distribution of the chosen sites colored by their respective plant functional types.

where f is the index over the characteristic frequencies. “Singular system analysis” (SSA, Golyandina et al., 2001; Ghil et al., 2002) is used to extract subsignals X_f . It has already been employed to explore daily eddy covariance ecosystem-biosphere fluxes (e.g. Mahecha et al., 2007, 2010a). The SSA method is used given that it could be easily applied to time series with gaps (Kondrashov and Ghil, 2006) and, other than many other methods, does not make any assumption on the shape of the subsignals. Here, the two steps of SSA are only summarized, while technical details can be found in the Appendix B of Mahecha et al. (2010a).

The decomposition of the time series comes as a first step. The idea is to embed the time lagged windows of the time series in its trajectory space. This embedding space can be decomposed into a set of empirical orthogonal functions and associated principal components (Ghil et al., 2002). Each component is characterized by one single oscillatory mode, and has a simple representation in the frequency domain.

The second step is the reconstruction of the time series through the principal components in the frequency domain. The original signal can be fully or partially reconstructed. This is a selective step, and the user has to decide which principal components are combined so that one can obtain a meaningful combination of principal components. It then promotes the concept of frequency binning.

In this study, we are interested in three prominent temporal patterns: diurnal, seasonal–annual and interannual. In order to reconstruct their respective variations, a fine resolution of the frequency binning scheme comprising 10 bins is firstly chosen a priori (Table 2). It should be noted that the chosen bin widths in this fine binning frequency scheme are sufficiently coarse to avoid misinterpretations due to inaccuracies occurring in the frequency assignments to the SSA modes (Mahecha et al., 2007). In this study, we considered diurnal variability as the sum of the principal components with dominant frequencies in the range of 7.9–41.6 h (Bin A), seasonal–annual as those in the range of 130–514 days (Bin B), and interannual as the sum of those with lower frequency (Bin C).

The hourly time series is used to reconstruct the diurnal variability. To improve computational efficiency of applying SSA, the full hourly time series is split into subsets with each one containing 60 days and a “local SSA” (Yiou et al., 2000; Table 2) is then applied to retrieve diurnal variability in each subset. It can be summarized as follows:

- Define continuous windows of length $W \ll N$ ($W = 1440$, covering 60 days) on the full hourly time series. The windows are centered on $0.5W, 1.5W, \dots, N - 0.5W$.
- Apply SSA on each window separately, and identify the diurnal component in each window based on Bin A (Table 2) and ignore the rest, such that it contains the diurnal variability.
- The local results are merged together.

For the characterization of seasonal–annual and interannual variability, a global SSA (Table 2) is performed on the daily time series aggregated from the hourly data. The reconstructions of

Table 2
Limits of the applied timescale binning schemes.

Global SSA		Local SSA	
Upper limit (day)	Lower limit (day)	Upper limit (h)	Lower limit (h)
Bin C		Maximum	
Maximum	513.7	218.8	218.8
Bin B		Bin A	
513.7	259.3	218.8	125.7
259.3	130.9	125.7	72.4
130.9	66.1	72.4	41.6
Bin A		Bin B	
66.1	33.4	41.6	23.9
33.4	16.9	23.9	13.8
16.9	8.5	13.8	7.9
8.5	4.3	7.9	4.6
4.3	2.2	4.6	2.6
2.2	Minimum	2.6	Minimum

The discretization for both global and local SSA is approximately equidistant in the log domain. Bin A, Bin B, and Bin C are used to reconstruct the time series characterized by diurnal, seasonal–annual and interannual variability, respectively. The bin boundaries (given in bold) could be decimal since they are approximately equally spaced over the logarithm of the frequencies.

seasonal–annual and interannual variability are based on Bin B and Bin C (Table 2), respectively.

Our site selection criteria allow limited data gaps in observed fluxes (maximum 30% gaps), but simulated fluxes are continuous. The data gap in both hourly and daily flux time series is filled by the SSA gap-filling procedure (c.f. Appendix B in Mahecha et al., 2010a). Note that the SSA gap-filling procedure would not be performed on the time series if its gap fraction is above 30%.

2.3.2. ANN error model

The ANN techniques are well adapted to solve nonlinear problems and are designed to capitalize on the inherent statistical relationships among the input and output variables. The type of ANN applied here is the feed-forward multilayer perceptron (MLP, Rumelhart et al., 1986) that allows for nonlinear mapping of sets of input data to a set of appropriate output. The nonlinear mapping model consists of nodes that are organized in three or more layers (an input layer and an output layer with one or more hidden layers). Any nodes, i and j in two consecutive layers are connected with synaptic weights w_{ij} determined by training the system (Melesse and Hanley, 2005). For each node in the hidden layer, it calculates a weighted sum of all of its inputs z_i following Eq. (2) and then uses a transfer function (hyperbolic tangent function $f(x) = \tanh(x)$ ranging from -1 to 1) to produce the output z_j of node j in the hidden layer following Eq. (3).

$$x_j = \sum_{i \in \text{Inputs}(j)} w_{ij} \cdot z_i \quad (2)$$

$$z_j = f(x_j) = f \left(\sum_{i \in \text{Inputs}(j)} w_{ij} \cdot z_i \right) \quad (3)$$

For the nodes in the output layer, the linear transfer function is used to calculate the output value.

In this study, we choose two hidden layers, each with five nodes. This choice is made to yield an accurate approximation of representations of state-dependent errors that may contain several “hills and valleys”, and two hidden layers with only several nodes have been proposed to work well compared to a single hidden layer requiring a large number of nodes (Chester, 1990; Zhang et al., 1998).

The target of ANN error modeling is ORCHIDEE errors, defined by the differences between modeled and observed fluxes, resulting in a vector containing hourly data. Training and evaluation of the ANN

is performed on ORCHIDEE errors (Fig. 2). The training phase determines the weights through establishing empirical relationships between ORCHIDEE errors and a combination of input predictors, including meteorological drivers and simulated ORCHIDEE flux. The parameterized ANN model with fixed weights after training is referred to ANN error model. The evaluation phase uses these weights (or ANN error model) to predict ORCHIDEE errors from the input predictors within a subset of the data (an evaluation dataset) that is not used for the training phase. In the evaluation dataset for each flux, the root mean square error reduction (RMSE-R), a metric to measure the transferability of state-dependent model bias (or error transferability), is then defined as:

$$\text{RMSE-R} = 1 - \frac{\sqrt{\sum_{i=1}^n \varepsilon_{\text{ANN}}^2}}{\sqrt{\sum_{i=1}^n \varepsilon_{\text{Ori}}^2}} \quad (4)$$

where ε_{ANN} and ε_{Ori} are ORCHIDEE errors with and without ANN-modeled, respectively.

In addition, all variables in both the input and output layers of ANN have been rescaled into a $[-1, 1]$ interval, and then the variable in the output layer has been scaled back to its original units before performing error calculations. ANN is not a robust extrapolation tool, for example, an ANN error model trained on the variable with one order of magnitude (e.g. interannual timescale) could be problematic in data extrapolation of another variable in an evaluation dataset with a higher order of magnitude (e.g. diurnal timescale). Multiple linear regression approach relating the ORCHIDEE errors to input predictors is also adopted to test error transferability between timescales.

The training procedure, which adjusts the connection weights of the network through error back-propagation based on the steepest descent method, is recognized as a crucial step in ANN error model framework. To avoid over-fitting, a 20% subset of the training dataset (the test dataset) is retained and used to assess the performance of the ANN training process at every stage of learning (Scardi, 2001). Training is stopped when the error within the test dataset begins to increase, i.e. the model starts to lose prediction or generalization ability by overtraining. The training procedure is also sensitive to how the training dataset is built and initial weights linking the nodes between the input layer and the first hidden layer (Abramowitz et al., 2007; Morshed and Kaluarachchi, 1998). To overcome these, we divide each variable (or node) in the input layer into different value ranges (or classes) according to its respective data distribution (e.g. van Wijk and Bouten, 1999), and then build the training set in such a way that it would randomly select the data from each class. 10 training sets are created in this way, and for each of 10 training sets, the ANN has been trained 5 times starting from different initial weights. In total, 50 ANNs have been trained and the mean ensemble is used.

2.3.3. Configurations of ANN error modeling

The original and reconstructed time series on three different characteristic timescales (diurnal, seasonal–annual and interannual) are used in the ANN error modeling. The ORCHIDEE errors from both original and reconstructed time series are then modeled by the ANN as a function of the drivers in their respective original and reconstructed forms. Note that the main purpose of this study is not to quantify the absolute value of state-dependent model bias but to understand the state-dependent model bias transferability in both spatial and temporal domains. Moreover, the choice of explanatory variables is constrained by the fact that a variable must be available at all EC sites. Thus, ANN inputs consist of three meteorological drivers (T_a : air temperature, VPD: vapor pressure deficit, R_g : incoming shortwave radiation) and the simulated ORCHIDEE flux. We use three instantaneous meteorological

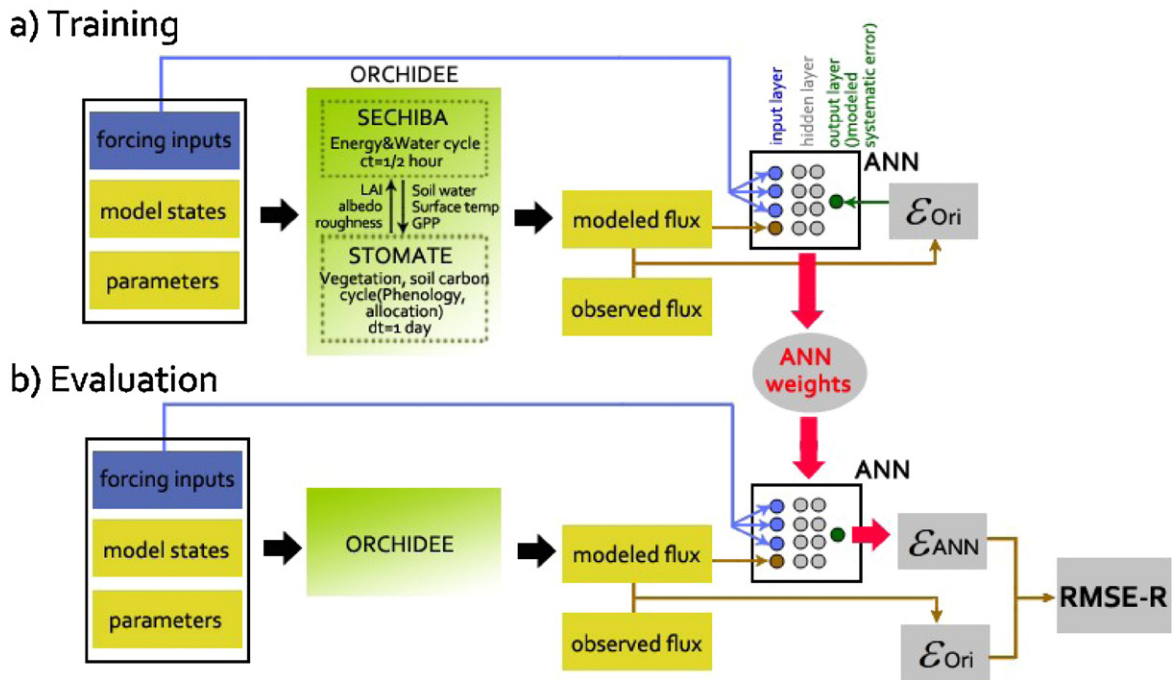


Fig. 2. The conceptual diagram of ANN operation. Two steps are involved in the ANN error modeling. (a) The training phase is to find a parameterized ANN error model with fixed weights (or nonlinear regression parameters) that characterize the relationships between ANN inputs and ANN output presented in training dataset and (b) the evaluation phase is to apply this ANN error model to compute ANN-modeled error and RMSE-R in the evaluation dataset.

inputs (T_a , VPD and R_g) because they explain the majority of the variation in modeled instantaneous carbon and water fluxes (van Wijk and Bouten, 1999, Moffat et al., 2010). However, this choice is arbitrary, and a systematic sensitivity study will be necessary to determine the optimal set of ANN inputs (Abramowitz et al., 2007), which should be explored in the future study. Other variables, such as diffuse PPF, soil temperature and soil moisture are not considered because they are not available for all sites. In addition, the soil depths at which soil temperature and moisture measurements have been made are not uniform across sites. To avoid any bias due to data gap filling methods by La Thuile FLUXNET data processing system (c.f. www.fluxdata.org) in computing ORCHIDEE errors, only time steps with actual measurements are used in the construction and the evaluation of the ANN error model.

The errors on five flux variables are investigated: sensible heat flux (H), latent heat flux (LE), gross primary productivity (GPP), ecosystem respiration (R_{eco}) and net ecosystem exchange of CO_2 (NEE). Note that GPP and R_{eco} are not measured directly. R_{eco} is modeled using the method of Reichstein et al. (2005) and GPP is then the absolute sum ($NEE + R_{eco}$). Therefore, any systematic errors in the flux-partitioning algorithm of Reichstein et al. (2005) could contribute to ORCHIDEE errors for these two gross fluxes. The ability of the ANN driven by meteorological variables and by the simulated ORCHIDEE flux to estimate RMSE-R for the following 8 configurations is examined:

Case WT: Transfer of ANN-modeled error within a timescale at each site. For example, at each site, using reconstructed time series on diurnal timescale, we train an ANN to model error on selected data from half of the time series and then use this error model to estimate RMSE-R in the remaining half. This is also performed upon the original time series. The number of sites is 125.

Case CT: Transfer of ANN-modeled error across timescales at each site. For example, at each site, using the reconstructed time series on diurnal timescale, we train an ANN error model on the entire time series, and then use this error model to estimate RMSE-R

on the entire reconstructed time series on both seasonal–annual and interannual timescales. The number of sites is 125.

Case S: Transfer of ANN-modeled error on the spatial scale (Table 3, climate group/PFT with at least 3 sites is considered).

Case S1: We train an ANN error model on the entire time series using two-thirds of the sites belonging to a class consisting of a specific PFT (e.g. grassland) and a specific climate group (e.g. temperate), and then apply this error model to estimate RMSE-R on the entire time series of the other one-third of the sites from the same class. This is a test of error spatial transferability within a PFT and a climate group. The number of classes is 15.

Case S2: We train an ANN error model on the entire time series using all sites belonging to a class consisting of a specific PFT (e.g. grassland) and a specific climate group (e.g. temperate), and then apply this error model to estimate RMSE-R on the entire time series of all sites belonging to a class consisting of the same PFT (e.g. grassland) but a different climate group (e.g. tropical). This is a test of error transferability within one PFT and between climate groups. The number of classes is 24.

Case S3: We train an ANN error model on the entire time series using all sites belonging to a class consisting of a specific PFT (e.g. grassland) and a specific climate group (e.g. temperate), and then

Table 3
Configurations of error transferability.

Case type	Full type name	Num. of classes
Case WT	Transferability within a timescale	125
Case CT	Transferability between timescales	125
Case S1	Spatial transferability within a PFT and a climate group	15
Case S2	Spatial transferability within a PFT and between climate groups	24
Case S3	PFT spatial transferability within a climate group	44
Case S4	Both PFT and climate group spatial transferability	210
Case S5	Spatial transferability within a PFT	7
Case S6	PFT spatial transferability	42

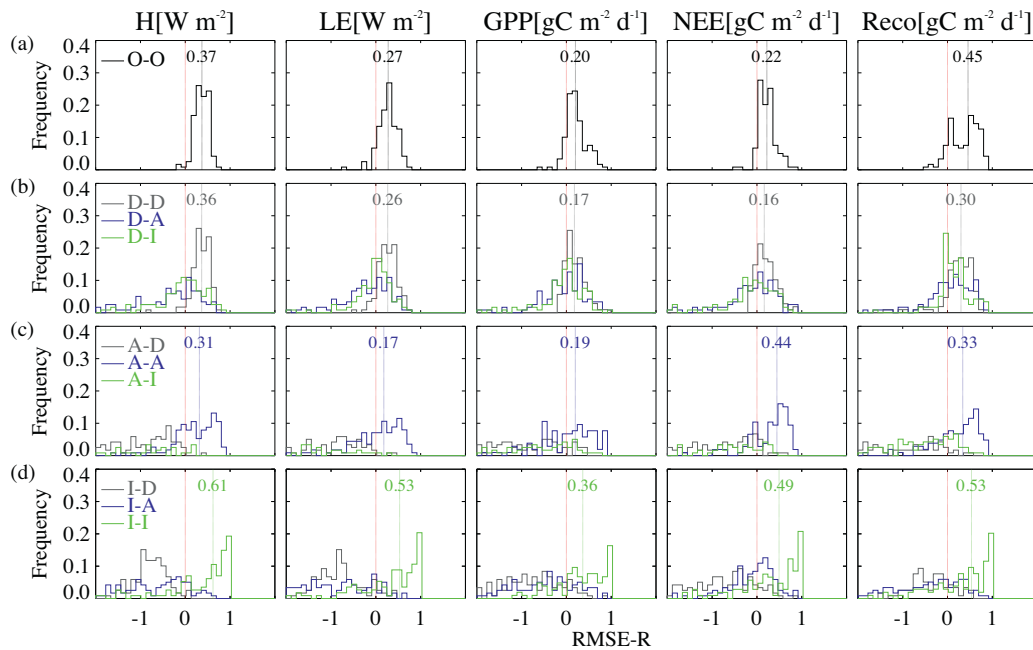


Fig. 3. The histogram of RMSE-R on the original time series (a: O-O), at three timescales (b: D-D, c: A-A and d: I-I) and across timescales (b: D-A and D-I; c: A-D and A-I; d: I-D and I-I) for H , LE , GPP , R_{eco} and NEE . O is the original time series, and D, A and I represent the reconstructed time series on diurnal, seasonal–annual and interannual timescales, respectively. An ANN error model is trained on one timescale (e.g. D) and then evaluated on another timescale (e.g. A) to get RMSE-R in A from D (D-A). The value on the graph represents the median value of the histogram of RMSE-R from 125 sites.

apply this error model to estimate RMSE-R on the entire time series of all sites belonging to a class consisting of a different PFT (e.g. cropland) but the same climate group (e.g. temperate). This is a test of PFT spatial transferability within each climate group. The number of classes is 44.

Case S4: We train an ANN error model on the entire time series using all sites belonging to a class consisting of a specific PFT (e.g. grassland) and a specific climate group (e.g. temperate), and then apply this error model to estimate RMSE-R on the entire time series of all sites belonging to a class consisting of a different PFT (e.g. cropland) and a different climate group (e.g. tropical). This is a test of both PFT and climate group spatial transferability. The number of classes is 210.

The error spatial transferability for the above four cases is investigated on both original and reconstructed time series with three characteristic timescales. In addition, we also investigate two additional cases of error spatial transferability based on the sites classified by PFT using the original time series.

Case S5: We train an ANN error model on the time series from two-third of all sites belonging to a specific PFT (e.g. grassland) and then apply this error model to estimate RMSE-R on the time series of the other third of sites from the same PFT. This is a test of spatial transferability within a PFT.

Case S6: We train an ANN error model on the entire time series from all sites belonging to a specific PFT (e.g. grassland) and then apply this error model to estimate RMSE-R on the entire time series of all sites from different PFT. This is a test of PFT spatial transferability.

ANN-modeled error in this study not only contains the errors originating from the model itself (or state-dependent model bias) but also include other systematic errors related to the flux measurements and data processing (e.g. Billesbach, 2011; Vickers et al., 2009, 2010). One of the potential sources of the error comes from a general lack of energy balance closure (Wilson et al., 2002; Foken, 2008; Leuning et al., 2012) at eddy covariance sites, where the observed turbulent fluxes of H and LE do not sufficiently account for the measured net available energy at the surface. Given that

the magnitude and causes of the failure to close energy balance varies among sites and timescales (e.g. Barr et al., 2006; Wilson et al., 2002; Foken et al., 2011), no corrections to the LE and H measurements are applied, in contrast to those performed in Jung et al. (2011). Fortunately, the data from the La Thuile FLUXNET dataset used in this study underwent a standardized preprocessing based on a friction velocity (u^*) filter and despiking of half hourly flux data (Papale et al., 2006). This procedure removes some systematic errors such as the ones which occur during calm nocturnal periods (Goulden et al., 1996). The errors related to the energy imbalance are therefore not necessarily the major source of the ANN-modeled errors. Richardson et al. (2007) have shown that random errors persist after this standardized preprocessing. However, this would not affect this analysis since our ANN-modeled errors do not contain any random errors. Thus, we might conclude that our ANN-modeled error can be mainly attributable to the model itself rather than to the observations. Such an assumption has also been supported by Abramowitz et al. (2007). However, the residual systematic errors from the observations cannot be easily disentangled from the ANN-modeled errors.

3. Results and discussion

3.1. RMSE-R on three different time scales (Case WT)

Fig. 3 shows RMSE-R for each flux variable within each timescale using ANN error modeling. All sites ($n=125$) are pooled to generate the histograms of RMSE-R for each flux at each timescale. As shown in Fig. 3, the interannual timescale is always associated with the largest RMSE-R (range of median values: 36–61%; which means that 36–61% of ORCHIDEE error in the evaluation dataset has been reduced by an ANN error model), and the diurnal timescale has the smallest RMSE-R (16–36%) and seasonal–annual timescale has the intermediate values (17–44%). This suggests that climate-dependent processes controlling fluxes are better represented by ORCHIDEE for short timescales than for long timescales. Previous studies have also noticed that land surface models tend to

fail in replicating interannual variations of carbon and water fluxes (Siqueira et al., 2006; Urbanski et al., 2007; Mahecha et al., 2010a; Keenan et al., 2012a). Climate has been recognized as an important driver of interannual variation in terrestrial fluxes (e.g. Hui et al., 2003; Sierra et al., 2009; Le Maire et al., 2010), and the model performance on long timescales would be significantly improved if its state-dependent model bias related to three meteorological variables (T_a , VPD and R_g) present in ANN error modeling could be removed by future model refinements.

The small RMSE-R on a diurnal timescale, particularly, for GPP and NEE reflects the ability of ORCHIDEE to resolve fast CO_2 exchange processes using theories related to canopy turbulent exchange, largely driven by radiation. On a diurnal cycle, both GPP and NEE have a lower RMSE-R than H , LE and R_{eco} . The higher state-dependent model bias in H can be expected because of the use of a single energy budget for both vegetation and soil (Krinner et al., 2005). The source of higher state-dependent model bias in R_{eco} can be related to the fact that the computation of heterotrophic respiration in ORCHIDEE is based on daily mean temperature, which suggests that decomposition rates are not well resolved. Another cause of concern is the unrealistic representation of soil carbon states in natural ecosystems, which is based on soil carbon equilibrium hypothesis when initializing soil carbon pools at the site level (Williams et al., 2009; Pietsch and Hasenauer, 2006; Wutzler and Reichstein, 2007; Carvalhais et al., 2008, 2010). However, there also exists the uncertainty in R_{eco} from La Thuile FLUXNET dataset since R_{eco} is separated from NEE using an empirical model (Reichstein et al., 2005). The observed high RMSE-R in H and LE could also be associated with unclosed surface energy balance (Wilson et al., 2002; Foken, 2008) and a general solution to this problem is still not available (Foken et al., 2011).

Our results suggest that only considering the state-dependent model bias in the original time series (range of median values: 20–45%) can mask relatively large residual state-dependent model biases on interannual (36–61%) timescales. Not separating timescale in model evaluations may thus lead to an optimistic assessment of model behavior on long timescales because of error cancelation across timescales (Mahecha et al., 2010a), that may also translate into flawed estimates of the carbon climate feedbacks (Wang et al., 2010; Mahecha et al., 2010b). We also found that the distribution of RMSE-R on interannual timescale is much more spread than other timescales, and one of the possibilities could be the accuracy of extracted interannual variability by SSA based on relatively short time series length in the La Thuile FLUXNET dataset. For example, Mahecha et al. (2010a) explored interannual timescale using the five-year time series of carbon and water fluxes and found that the uncertainty of subsignal separation is very large, which did not allow accurate assessment of interannual variability. This emphasized the necessity of continued flux monitoring for the understanding of the longer-term carbon and water flux variability, and the use of other long-term variables such as basal area growth from tree ring records (Briffa et al., 2008).

To determine the fraction of state-dependent errors that could be accounted for by an ANN error model based on original time series, we made a comparison between RMSE in the fluxes after ANN error modeling and the random flux errors in a temperate deciduous forest site at the Howland temperate evergreen needleleaf forest site. The random flux errors were estimated by comparing the results of two eddy covariance towers installed near one another during the year 2000 (Hollinger and Richardson, 2005) (Table 4). This comparison shows that the RMSE after applying an ANN error model remains more than two times larger in absolute value than the random flux errors (Table 4). For example, ANN error modeling can strongly reduce the RMSE of yearly H (W m^{-2}), LE (W m^{-2}) and NEE ($\mu\text{mol m}^{-2} \text{s}^{-1}$) RMSE (to 45.8,

43.2 and 3.18). But the residual RMSE is still higher than the corresponding random flux errors (19.5, 16.5 and 1.5) (Table 4). This might be related to the fact that considering only climate drivers as ANN input variables is inadequate. Other variables could be important, such as delayed response to external forcings (e.g. van der Molen et al., 2011), or soil moisture and management activities (crop rotations, irrigation, fertilization) for crops and managed forests (e.g. Jaksic et al., 2006; Peichl et al., 2011; Smith et al., 2010). In Howland, for example, the inclusion of soil temperature as another ANN driver, an input recognized as an important regulator of carbon exchange during soil thawing in that forest ecosystem (Hollinger et al., 1999), can further reduce the RMSE in NEE by 5% (Table 4). It should be noted that the random flux errors could vary between sites, such that the fraction of systematic errors accounted for by the ANN error model is site-dependent. But the state-dependent model bias removed in this study might be beyond the random flux errors on most of EC sites, since ANN input drivers could be limited by both data availability and our understanding of the underlying processes.

3.2. Error transferability across different timescales (Case CT)

To investigate whether ANN-modeled errors are transferable across different timescales, we examine whether the ANN error model constructed at one timescale could be useful to reduce ORCHIDEE errors on other timescales. Fig. 3b–d shows that it is not the case. Indeed, there is a near zero or even negative median RMSE-R (meaning a decrease in the fit of the data to the ANN error model) (Fig. 3b–d), and also a widening of the frequency of RMSE-R, indicating different results across sites. This is also confirmed if ORCHIDEE errors were related to the input predictors by multiple linear regression approach rather than ANN (data not shown). Moreover, poor error transferability across timescales has been documented in other studies. For example, Siqueira et al. (2006) demonstrated that the model employed for resolving fast CO_2 and H_2O exchange processes using theories related to canopy turbulent exchange could not necessarily translate into improved predictive skills for long timescales. Mahecha et al. (2007) also showed that a clear hysteresis between seasonal–annual components of NEE (photosynthesis, autotrophic and heterotrophic respiration) and air temperature is significantly affected by adding the interannual component to the seasonal–annual cycle. This leads potentially to a different response of NEE to temperature on different timescales. Poor cross-timescale transferability of state-dependent model biases for ORCHIDEE found in this study also implies that this model can capture most of timescale-independent behaviors in ecosystem flux simulations (Baldocchi et al., 2001; Katul et al., 2001; Stoy et al., 2009) or that there is little interactions between timescales for the state-dependent model biases, though large RMSE-R still existed when transferring errors within seasonal–annual or interannual timescales as mentioned in Section 3.1.

3.3. Error spatial transferability (Case S)

3.3.1. Original time series

In Abramowitz et al. (2007), only two different PFTs and 13 eddy covariance sites were used to investigate the spatial transferability of ANN-modeled errors. In this study, this approach is extended through involving 125 sites distributed across 7 PFTs. For different fluxes, the median RMSE-R from all classes in both Case S5 (spatial transferability within a PFT, $n = 7$) and Case S6 (PFT spatial transferability, $n = 42$) are displayed in the diagonal and non-diagonal terms of the matrix in Fig. 4, respectively. Case S5 analysis suggested that the median RMSE-R in H (W m^{-2}), LE (W m^{-2}), GPP ($\text{g C m}^{-2} \text{d}^{-1}$),

Table 4
Measurements of random flux errors, RMSE (root mean square error) of simulated ORCHIDEE flux variables and their ANN-modeled values during the year 2000 in Howland forest.

Flux variable	Howl. 2 tower	ORCHIDEE	ANN1	ANN2	(ANN1 – ANN2)/ANN1 (%)
H (W m^{-2})	19.5	129.1	45.8	45.3	1.1
LE (W m^{-2})	16.5	73.9	43.2	42.1	2.5
NEE ($\mu\text{mol m}^{-2} \text{s}^{-1}$)	1.5	4.93	3.18	3.02	5.0

Howl. 2 tower data from the experiment reported by Hollinger and Richardson (2005), where random errors are estimated using simultaneous measurements from two flux towers separated by around 775 m. ANN1 is the root mean square error of the ANN model with air temperature, global radiation, vapor pressure deficit and modeled output as drivers; ANN2 is the same with ANN1 but with soil temperature in surface layer as another driver.

R_{eco} ($\text{g C m}^{-2} \text{d}^{-1}$) and NEE ($\text{g C m}^{-2} \text{d}^{-1}$) is of 36, 32, 18, 43 and 19%, respectively. For GPP and NEE, cropland (32 and 34%) and BoENF (33 and 27%) have the highest RMSE-R in Case S5. For the cropland which covers any kind of cultivated species, this can be expected since the parameterization used for crop in ORCHIDEE is similar to the one used for herbaceous vegetation, and does not account for management practices and crop variety-dependent parameters (Smith et al., 2010; Li et al., 2011). Case S6 analysis (PFT spatial transferability) suggests that most of RMSE-R in H, LE and R_{eco} across PFTs are positive (Fig. 4), indicating that ANN error modeling does improve the prior ORCHIDEE model simulation. This was also found by Abramowitz et al. (2007) when comparing H and LE across grassland and conifers for all of the land surface models they considered. By contrast, the picture of RMSE-R between PFTs in GPP and NEE is different. For example, based on the constructed ANN error model in TrEBF, ANN produces a marginal or negative RMSE-R in GPP for the other PFTs (Fig. 4; that is degradation from the prior ORCHIDEE simulation).

3.3.2. Different timescales

As shown in the whisker boxes of Fig. 5, the median RMSE-R from all classes in Case S1 (spatial transferability within a PFT and a climate group, $n = 15$) is always positive at all timescales for each flux variable. The comparison between Case S1 on the Y-axis and other cases on the X-axis (Case 2: $n = 24$, Case 3: $n = 44$ and Case 4: $n = 210$) is also shown in Fig. 5. The 1:1 line (Fig. 5) showed that the median RMSE-R in Case S1 ($n = 15$) is larger than those from other cases on each timescale. The RMSE-R is often negative (that is the model misfit increased after applying the ANN error model) or near zero on seasonal–annual and interannual timescales in all cases except Case S1. On the diurnal timescale, the median RMSE-R of all classes within each case is positive for all flux variables. This is comparable to the ANN error model applied on the original time series (Fig. 5). This can be expected due to the fact that diurnal timescale carries the largest spectral power among the three characteristic timescales and most of the variability in the original time series can be accounted for by the diurnal timescale part.

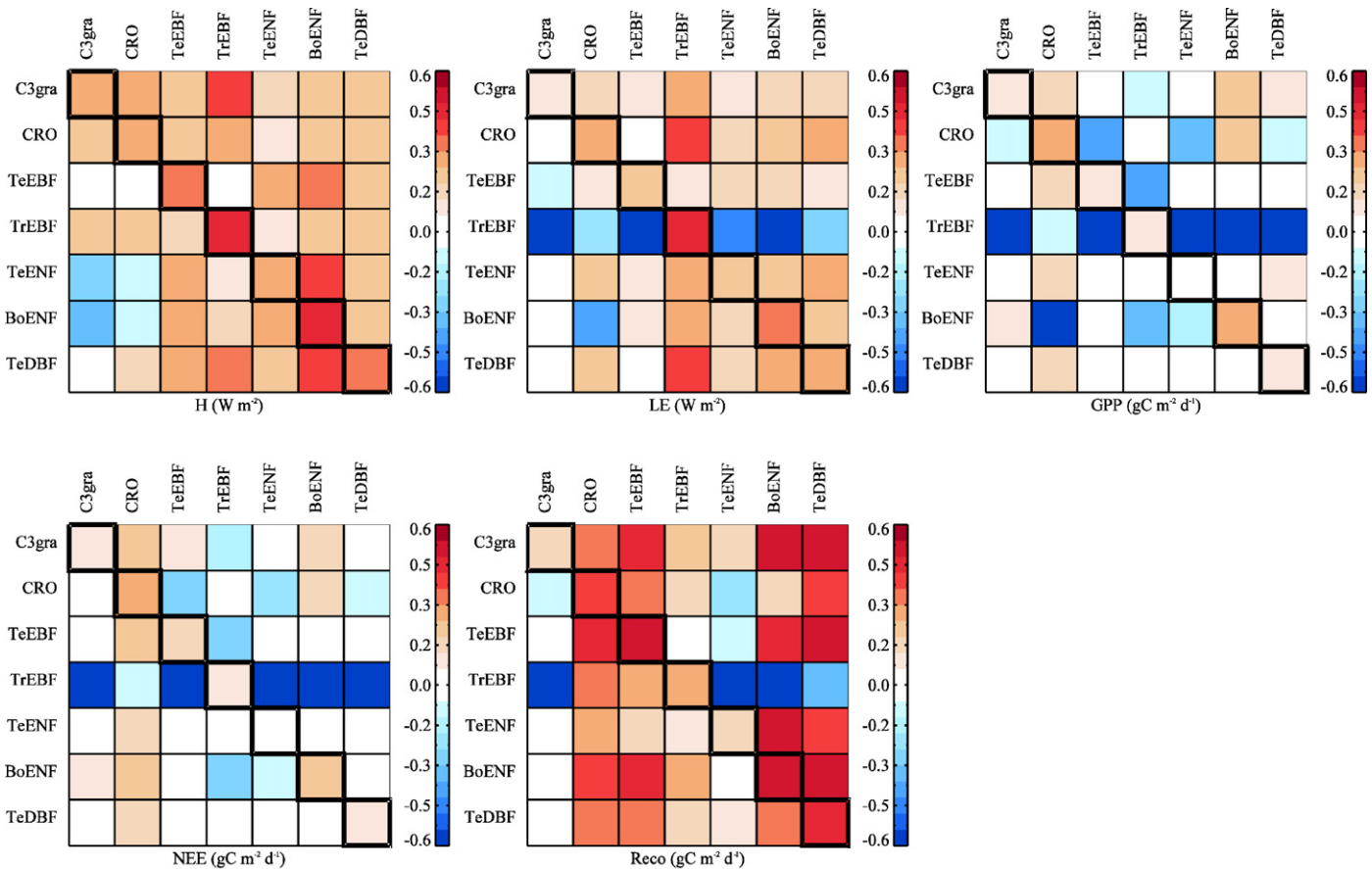


Fig. 4. Matrix of the median RMSE-R from all classes in both Case S5 (diagonal) and Case S6 (non-diagonal) for H, LE, NEE, GPP and R_{eco} . An ANN error model is trained on the vertical PFT (e.g. CRO) and then evaluated on the horizontal PFT (e.g. TeENF) to get RMSE-R in TeENF from CRO.

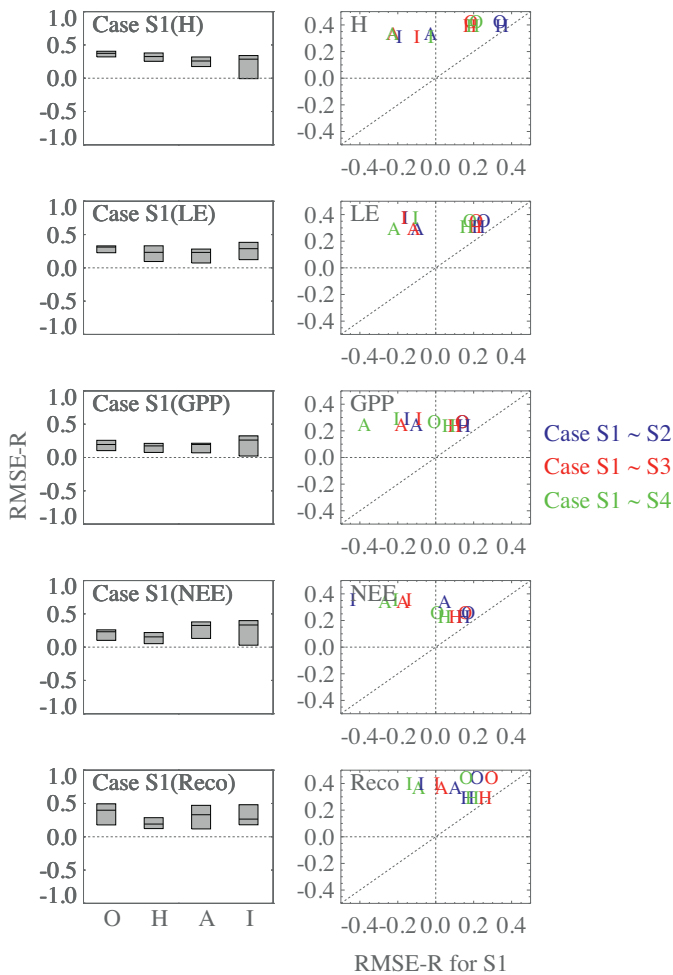


Fig. 5. The whisker box of RMSE-R in Case S1 for *H*, *LE*, *GPP*, *R_{eco}* and *NEE* on the original time series and reconstructed time series at three different characteristic timescales. The scatter plots for Case S2 vs. Case S1, Case S3 vs. Case S1 and Case S4 vs. Case S1 are also shown. O, H, A and I represent the original time series, reconstructed time series at diurnal, seasonal–annual and interannual timescales, respectively. The whisker box is consisted of median value (solid line), 25 and 75% of the data.

Firstly, Case S1 analysis suggested that ANN-modeled error is transferable within a PFT and within a climate group at all timescales. This means that each PFT/climate group has specific features that the model is not able to reproduce, and thus suggests that better model performances could be achievable by improving the parameterization at the level of PFT/climate group. The result implies that model improvement based on specific eddy covariance sites can indeed enhance the model behavior at other sites within the same PFT and the same climate group. This is a key result showing the non-local character of eddy-flux point-scale observations to improve the description of fluxes through process-based modeling. It provides evidence for mapping carbon fluxes, for example, using tower flux data in different PFT/climate combinations as priors in an inverse modeling framework (e.g. Göckede et al., 2010; Jung et al., 2011). Theoretically, the information on error transferability in a PFT and climate group could also be used to optimize the future network designed for carbon and water studies through better locating the sites for a given model.

Secondly, the ANN-modeled errors are less transferable between sites belonging to different climate groups (Case S2 and S3) and different PFTs (Case S3 and S4) especially on the seasonal–annual and interannual timescales, as shown by the reduced or negative error transferability e.g. in *LE* and *NEE* (Fig. 5).

This indicates that the method used to discretize vegetation types in ORCHIDEE cannot fully describe the representation of ecosystem functioning on the long timescale. The ORCHIDEE model would benefit from accounting for more detailed climate groups in addition to PFTs for its parameterization. This is similar to results from field observations on hundreds of plots showing ecoregion (primarily delimited by climate, e.g. seasonal high and low temperatures, precipitation) differences in forest type productivity, carbon pools, and recovery from disturbance for a given forest type (Hudiburg et al., 2009).

Thirdly, between sites (Case S2–S4), positive error transferability is found on the diurnal timescale and original time series instead of long timescales. The ANN-modeled errors on the short timescale are much less sensitive to PFT or climate group than the errors on the long timescales, which is notably for *H*, *LE* and *R_{eco}* (Fig. 5). However, this does not mean that the model has a better ability to characterize the main processes driving the fluxes on long timescales. In fact, larger relative model–observation mismatch have been observed on long timescales (seasonal–annual and interannual) compared to short timescales (diurnal). One of the reasons is that on the diurnal cycle, the processes of photosynthesis and respiration are largely instantaneous responses to diurnal climate variability (i.e. solar radiation, air temperature and humidity) (Baldocchi, 1997). While, the long timescales might be more affected by climate through site-specific slowly varying ‘biotic’ variables (e.g. phenology, soil carbon, leaf area, carbon allocation) (Richardson et al., 2007; Stoy et al., 2009; Jung et al., 2011; Dietze et al., 2011; Keenan et al., 2012b), land use and disturbance history (Law et al., 2004), fertility and delayed responses to environmental variations (Schimel et al., 2005). However, we should be informed of the inaccuracy of the extracted interannual variability by SSA using relatively short time series in La Thuile FLUXNET dataset (see Section 3.1).

4. Conclusions and outlooks

Our study develops and applies a neural network-based technique combined with time series decomposition to explore the transferability of state-dependent model biases in both spatial and timescale domains. This could enable the land surface modeling community to identify a theoretical bound for the space of model improvement and model uncertainties reduction. The positive error transferability is always found on both diurnal cycle and original time series instead of long timescales (seasonal–annual and interannual). Meanwhile, processes influencing fluxes vary with timescales (the carbon allocation, phenology, carry-over effects from anomalous climate years and disturbances), which can be characterized by the near-zero or even negative error transferability across timescales. Our study implies that the model development aimed to reduce model–observation mismatch using original time series mostly benefits the short timescale (e.g. diurnal cycle) instead of long timescales, because short timescale often accounts for most of the variability in original time series. Thus, model evaluation and development should pay particular attention to the representation of processes across timescales to avoid state-dependent biases at longer timescales.

Utilizing the global eddy covariance network, our study is the first to examine the error transferability across sites in a large spatial domain, which is delimited by PFT and climate groups. The flux data represent ecosystem-scale processes and along with site meteorology, provide a means to diagnose model performance over a range of temporal scales. This analysis showed that model improvement achieved on the sites in a specific PFT and a specific climate group could translate into improved model simulations at other sites belonging to the same PFT and the same climate group. This

is a non-local character of eddy flux point observations to improve flux simulations through process-based modeling.

It should be noted that the state-dependent model biases are only partially characterized in this study, because ANN inputs could be restricted by both data availability and poor understanding of some underlying processes. Meanwhile, long timescale separation from the original time series by SSA is unstable, and long-term eddy covariance records are thus needed, since they would facilitate the improvement of the representation of inter-annual variability in current land surface models. As longer records of fluxes and the measurement of other variables such as moisture become available for large sets of sites (e.g. Zreda et al., 2012), these methods may be regarded as promising for diagnosing model weaknesses and prioritizing improvements to the models. Our results are built upon ORCHIDEE and it will be interesting to know whether our conclusions on error transferability are robust across different land surface models in the future study.

Acknowledgements

The authors would like to thank all the PIs of eddy covariance sites, technicians, postdoctoral fellows, research associates and site collaborators involved in FLUXNET who are not included as co-authors of the paper, without whose work this meta-analysis would not be possible. This work is the outcome of the La Thuile FLUXNET workshop 2007, which would not have been possible without the financial support provided by CarboEurope-IP, FAO-GTOS-TCO, iLEAPS, Max Planck Institute for Biogeochemistry, National Science Foundation, University of Tuscia and the US Department of Energy. This research was supported by the Office of Science (BER), U.S. Department of Energy for the development of measurement standards, quality assurance, and data management protocols for AmeriFlux and Fluxnet. The Berkeley Water Center, Lawrence Berkeley National Laboratory, Microsoft Research eScience, Oak Ridge National Laboratory provided databasing and technical support. The AmeriFlux, AfriFlux, AsiaFlux, CarboAfrica, CarboEuropeIP, ChinaFlux, Fluxnet-Canada, KoFlux, LBA, NECC, OzFlux, TCOS-Siberia, and USCCC networks provided data. We would also acknowledge the PhD funding by Commissariat à l'énergie atomique (CEA) in France.

Appendix A. ORCHIDEE climate forcing data gap filling algorithms

For off-line simulations ORCHIDEE requires continuous half-hourly incoming shortwave radiation (W m^{-2}), incoming longwave radiation (W m^{-2}), air temperature (K), specific humidity (kg kg^{-1}), wind speed (m s^{-1}), surface pressure (Pa), and precipitation rate ($\text{kg m}^{-2} \text{s}^{-1}$). Before gap-filling, all half-hourly data in La Thuile FLUXNET synthesis dataset is aggregated to daily values. Each daily gap present in the climate forcing at eddy covariance site is replaced by the corrected daily data from ECMWF ERA-Interim (IERA) 0.7×0.7 degree reanalysis. For all variables, the correction applied to daily IERA fields was made by performing a linear regression analysis between daily in situ and IERA data. Since climate forcing in ORCHIDEE is defined at a half-hourly time step, a diurnal cycle for each climate variable should be rebuilt from their daily values. The following algorithm for disaggregating daily field to the half-hourly one only applies to the gap-filled daily values.

For air temperature, half-hourly temperature values in gaps are generated from daily values of maximum and minimum air temperature by using a sinusoidal function assuming that maximum temperature occurs at 14:00 local time and minimum temperature occurs at sunrise (Campbell and Norman, 1998). Half-hourly specific humidity values are given by half-hourly dew point temperature values. The latter is computed from the interpolated air temperature minus the difference between mean daily dew point temperature and mean daily air temperature. The diurnal cycle of incoming shortwave radiation is assumed to fit a second-order polynomial during daytime with a maximum at noon, and is set to zero before sunrise and after sunset. The incoming longwave radiation is computed at a half-hourly time step from air temperature, air humidity, and incoming shortwave radiation according to Crawford and Duchon (1999). Half-hourly wind speed is obtained by a logarithmic function of both daily value and independent random number generated from the normal distribution (Nicks et al., 1987). For surface pressure, a constant value is assumed throughout the day. Daily precipitation amounts are converted to half-hourly by evenly distributing precipitation throughout the day.

Appendix B.

Table B1.

Table B1

List of site ID, latitude, longitude, PFT and climate of the sites used in the analysis.

Site ID	Latitude	Longitude	PFT	Climate group	References
AT-Neu	47.12	11.32	GRA	Temperate	Wohlfahrt et al. (2008)
AU-Tum	−35.66	148.15	TeEBF	Temperate	
AU-Wac	−37.43	145.19	TeEBF	Temperate	
BE-Bra	51.31	4.52	TeDBF	Temperate	
BE-Lon	50.55	4.74	CRO	Temperate	
BE-Vie	50.31	6	TeDBF	Temperate	Aubinet et al. (2001)
BR-Ban	−9.82	−50.16	TrEBF	Tropical	
BR-Cax	−1.72	−51.46	TrEBF	Tropical	
BR-Ji2	−10.08	−61.93	TrEBF	Tropical	
BR-Ma2	−2.61	−60.21	TrEBF	Tropical	
BR-Sa1	−2.86	−54.96	TrEBF	Tropical	
BR-Sa3	−3.02	−54.97	TrEBF	Tropical	
CA-Ca1	49.87	−125.33	TeENF	Temperate	Humphreys et al. (2006)
CA-Ca2	49.87	−125.29	TeENF	Temperate	Humphreys et al. (2006)
CA-Ca3	49.53	−124.9	TeENF	Temperate	
CA-Gro	48.22	−82.16	TeDBF	Temperate-Continental	McCaughey et al. (2006), Pejam et al. (2006), Thomas et al. (2011)
CA-Let	49.71	−112.94	GRA	Temperate-Continental	Flanagan et al. (2002), Flanagan and Johnson (2005)
CA-Man	55.88	−98.48	BoENF	Boreal	Dunn et al. (2007)
CA-NS1	55.88	−98.48	BoENF	Boreal	
CA-NS2	55.91	−98.52	BoENF	Boreal	
CA-NS3	55.91	−98.38	BoENF	Boreal	
CA-NS4	55.91	−98.38	BoENF	Boreal	
CA-Obs	53.99	−105.12	BoENF	Boreal	
CA-Ojp	53.92	−104.69	BoENF	Boreal	Kljun et al. (2006)
CA-Qcu	49.27	−74.04	BoENF	Boreal	Giasson et al. (2006)
CA-Qfo	49.69	−74.34	BoENF	Boreal	Bergeron et al. (2007)
CA-SF1	54.49	−105.82	BoENF	Boreal	Mkhabela et al. (2009)
CA-SF2	54.25	−105.88	BoENF	Boreal	Mkhabela et al. (2009)
CA-SF3	54.09	−106	BoENF	Boreal	Mkhabela et al. (2009)
CA-SJ1	53.91	−104.66	BoENF	Boreal	
CA-SJ2	53.95	−104.65	BoENF	Boreal	
CA-TP2	42.77	−80.46	TeENF	Temperate-Continental	Peichl and Arain (2007)
CA-TP3	42.71	−80.35	TeENF	Temperate-Continental	Peichl and Arain (2007)
CA-TP4	42.71	−80.36	TeENF	Temperate-Continental	Arain and Restrepo-Coupe (2005)
CH-Oe1	47.29	7.73	GRA	Temperate	Ammann et al. (2007)
CZ-BK1	49.5	18.54	TeENF	Temperate-Continental	
CZ-BK2	49.5	18.54	GRA	Temperate-Continental	
DE-Bay	50.14	11.87	TeENF	Temperate	Staudt and Foken (2007)
DE-Geb	51.1	10.91	CRO	Temperate	Kutsch et al. (2010b)
DE-Hai	51.08	10.45	TeDBF	Temperate	Knohl et al. (2003), Kutsch et al. (2010a)
DE-Kli	50.89	13.52	CRO	Temperate	
DE-Meh	51.28	10.66	GRA	Temperate	Don et al. (2009)
DE-Tha	50.96	13.57	TeENF	Temperate	Grunwald and Bernhofer (2007)
DE-Wet	50.45	11.46	TeENF	Temperate	Rebmann et al. (2010)
DK-Sor	55.49	11.65	TeDBF	Temperate	Pilegaard et al. (2003)
ES-ES1	39.35	−0.32	TeENF	SubTropical-Mediterranean	
ES-ES2	39.28	−0.32	CRO	SubTropical-Mediterranean	
ES-VDA	42.15	1.45	GRA	Temperate	
FI-Hyy	61.85	24.29	BoENF	Boreal	Suni et al. (2003b)
FI-Sod	67.36	26.64	BoENF	Boreal	Suni et al. (2003a), Thum et al. (2009)
FR-Hes	48.67	7.06	TeDBF	Temperate	Granier et al. (2000)
FR-LBr	44.72	−0.77	TeENF	Temperate	Berbigier et al. (2001)
FR-Lq1	45.64	2.74	GRA	Temperate	
FR-Lq2	45.64	2.74	GRA	Temperate	
FR-Pue	43.74	3.6	TeEBF	SubTropical-Mediterranean	
GF-Guy	5.28	−52.93	TrEBF	Tropical	Bonal et al. (2008)
HU-Bug	46.69	19.6	GRA	Temperate	
HU-Mat	47.85	19.73	GRA	Temperate	
IE-Ca1	52.86	−6.92	CRO	Temperate	
IE-Dri	51.99	−8.75	GRA	Temperate	Byrne et al. (2007)
IS-Gun	63.83	−20.22	TeDBF	Temperate	
IT-Amp	41.9	13.61	GRA	SubTropical-Mediterranean	Gilmanov et al. (2007)
IT-BCi	40.52	14.96	CRO	SubTropical-Mediterranean	Kutsch et al. (2010b)
IT-Col	41.85	13.59	TeDBF	SubTropical-Mediterranean	
IT-Cpz	41.71	12.38	TeEBF	SubTropical-Mediterranean	Garbulsky et al. (2008)
IT-LMa	45.58	7.15	GRA	Temperate	
IT-Lav	45.96	11.28	TeENF	Temperate	
IT-MBo	46.02	11.05	GRA	Temperate	Marcolla and Cescatti (2005), Gianelle et al. (2009)
IT-Mal	46.12	11.7	GRA	Temperate	
IT-Non	44.69	11.09	TeDBF	SubTropical-Mediterranean	
IT-PT1	45.2	9.06	TeDBF	SubTropical-Mediterranean	Migliavacca et al. (2009)
IT-Ren	46.59	11.43	TeENF	Temperate	Montagnani et al. (2009)
IT-Ro1	42.41	11.93	TeDBF	SubTropical-Mediterranean	Rey et al. (2002)
IT-Ro2	42.39	11.92	TeDBF	SubTropical-Mediterranean	Tedeschi et al. (2006)
IT-SRo	43.73	10.28	TeENF	SubTropical-Mediterranean	
JP-Tak	36.15	137.42	TeDBF	Temperate-Continental	

Table B1 (Continued)

Site ID	Latitude	Longitude	PFT	Climate group	References
JP-Tom	42.74	141.51	TeDBF	Temperate-Continental	
KR-Hnm	34.55	126.57	CRO	SubTropical-Mediterranean	
KR-Kw1	37.75	127.16	TeDBF	Temperate-Continental	
NL-Ca1	51.97	4.93	GRA	Temperate	
NL-Hor	52.03	5.07	GRA	Temperate	
NL-Loo	52.17	5.74	TeENF	Temperate	Dolman et al. (2002)
PT-Esp	38.64	-8.6	TeEBF	SubTropical-Mediterranean	
PT-Mi1	38.54	-8	TeEBF	SubTropical-Mediterranean	
PT-Mi2	38.48	-8.02	GRA	SubTropical-Mediterranean	
RU-Che	68.61	161.34	GRA	Boreal	Merbold et al. (2009)
RU-Fyo	56.46	32.92	TeENF	Temperate-Continental	Milyukova et al. (2002)
RU-Ha1	54.73	90	GRA	Boreal	Marchesini et al. (2007)
RU-Zot	60.8	89.35	BoENF	Boreal	
SE-Fla	64.11	19.46	BoENF	Boreal	
SE-Nor	60.09	17.48	TeENF	Temperate-Continental	
UK-ESa	55.91	-2.86	CRO	Temperate	
US-ARM	36.61	-97.49	CRO	SubTropical-Mediterranean	
US-Bkg	44.35	-96.84	GRA	Temperate-Continental	Gilmanov et al. (2005)
US-Blo	38.9	-120.63	TeENF	SubTropical-Mediterranean	
US-Bo1	40.01	-88.29	CRO	Temperate-Continental	Meyers and Hollinger (2004)
US-Bo2	40.01	-88.29	CRO	Temperate-Continental	Meyers and Hollinger (2004)
US-Dk1	35.97	-79.09	GRA	SubTropical-Mediterranean	
US-Dk2	35.97	-79.1	TeDBF	SubTropical-Mediterranean	
US-Dk3	35.98	-79.09	TeENF	SubTropical-Mediterranean	
US-Goo	34.25	-89.97	GRA	SubTropical-Mediterranean	
US-Ha1	42.54	-72.17	TeDBF	Temperate-Continental	Urbanski et al. (2007)
US-Ho1	45.2	-68.74	TeENF	Temperate-Continental	Hollinger et al. (2004)
US-Ho2	45.21	-68.75	TeENF	Temperate-Continental	
US-IB1	41.86	-88.22	CRO	Temperate-Continental	
US-IB2	41.84	-88.24	GRA	Temperate-Continental	
US-LPH	42.54	-72.18	TeDBF	Temperate-Continental	Borken et al. (2006)
US-MMS	39.32	-86.41	TeDBF	SubTropical-Mediterranean	Schmid et al. (2000)
US-MOz	38.74	-92.2	TeDBF	SubTropical-Mediterranean	
US-Me2	44.45	-121.56	TeENF	SubTropical-Mediterranean	Thomas et al. (2009)
US-Me4	44.5	-121.62	TeENF	SubTropical-Mediterranean	Law et al. (2001)
US-Ne1	41.17	-96.48	CRO	Temperate-Continental	Verma et al. (2005)
US-Ne2	41.16	-96.47	CRO	Temperate-Continental	Verma et al. (2005)
US-Ne3	41.18	-96.44	CRO	Temperate-Continental	Verma et al. (2005)
US-PFa	45.95	-90.27	TeDBF	Temperate-Continental	Ricciuto et al. (2008)
US-SP2	29.76	-82.24	TeENF	SubTropical-Mediterranean	
US-SP3	29.75	-82.16	TeENF	SubTropical-Mediterranean	
US-Syv	46.24	-89.35	TeDBF	Temperate-Continental	Desai et al. (2005)
US-UMB	45.56	-84.71	TeDBF	Temperate-Continental	Gough et al. (2008)
US-Var	38.41	-120.95	GRA	SubTropical-Mediterranean	Ma et al. (2007)
US-WBW	35.96	-84.29	TeDBF	SubTropical-Mediterranean	
US-WCr	45.81	-90.08	TeDBF	Temperate-Continental	Cook et al. (2004)
US-Wi4	46.74	-91.17	TeENF	Temperate-Continental	
US-Wrc	45.82	-121.95	TeENF	SubTropical-Mediterranean	
VU-Coc	-15.44	167.19	TrEBF	Tropical	

The definitions of different PFTs are: boreal evergreen needleleaf forest (BoENF), temperate evergreen needleleaf forest (TeENF), temperate evergreen broadleaf forest (TeEBF), temperate deciduous broadleaf forest (TeDBF), grasslands (GRA), croplands (CRO), tropical evergreen broadleaf forest (TrEBF).

References

- Abramowitz, G., Pitman, A., Gupta, H., Kowalczyk, E., Wang, Y.P., 2007. Systematic bias in land surface models. *Journal of Hydrometeorology* 8, 989–1001.
- Abramowitz, G., 2005. Towards a benchmark for land surface models. *Geophysical Research Letters* 32.
- Ammann, C., Flechard, C.R., Leifeld, J., Neftel, A., Fuhrer, J., 2007. The carbon budget of newly established temperate grassland depends on management intensity. *Agriculture Ecosystems & Environment* 121, 5–20.
- Arain, A.A., Restrepo-Coupe, N., 2005. Net ecosystem production in a temperate pine plantation in southeastern Canada. *Agricultural and Forest Meteorology* 128, 223–241.
- Aubinet, M., Chermanne, B., Vandenhaute, M., Longdoz, B., Yernaux, M., Laitat, E., 2001. Long term carbon dioxide exchange above a mixed forest in the Belgian Ardennes. *Agricultural and Forest Meteorology* 108, 293–315.
- Baldocchi, D., 1997. Measuring and modelling carbon dioxide and water vapour exchange over a temperate broad-leaved forest during the 1995 summer drought. *Plant Cell and Environment* 20, 1108–1122.
- Baldocchi, D., 2008. Breathing of the terrestrial biosphere: lessons learned from a global network of carbon dioxide flux measurement systems. *Australian Journal of Botany* 56, 1–26.
- Baldocchi, D.D., Falge, E., Gu, L., Olson, R., Hollinger, D., Running, S., Anthoni, P., Bernhofer, Ch., Davis, K., Fuentes, J., Goldstein, A., Katul, G., Law, B.E., Lee, X., Mahli, Y., Meyers, T., Munger, W., Oechel, W., Paw U, K.T., Pilegaard, K., Schmid, H.P., Valentini, R., Verma, S., Vesala, T., Wilson, K., Wofsy, S.W., 2001. FLUXNET: A new tool to study the temporal and spatial variability of ecosystem-scale carbon dioxide, water vapor and energy flux densities. *Bulletin of the American Meteorological Society* 82, 2415–2434.
- Barr, A.G., Morgenstern, K., Black, T.A., McCaughey, J.H., Nestic, Z., 2006. Surface energy balance closure by the eddy-covariance method above three boreal forest stands and implications for the measurement of the CO₂ flux. *Agricultural and Forest Meteorology* 140, 322–337.
- Berbigier, P., Bonnefond, J.M., Mellmann, P., 2001. CO₂ and water vapour fluxes for 2 years above Euroflux forest site. *Agricultural and Forest Meteorology* 108, 183–197.
- Bergeron, O., Margolis, H.A., Black, T.A., Coursolle, C., Dunn, A.L., Barr, A.G., Wofsy, S.C., 2007. Comparison of carbon dioxide fluxes over three boreal black spruce forests in Canada. *Global Change Biology* 13, 89–107.
- Billesbach, D.P., 2011. Estimating uncertainties in individual eddy covariance flux measurements: a comparison of methods and a proposed new method. *Agricultural and Forest Meteorology* 151, 394–405.
- Bonal, D., Bosc, A., Ponton, S., Goret, J.-Y., Burban, B., Gross, P., Bonnefond, J.-M., Elbers, J., Longdoz, B., Epron, D., Guehl, J.-M., Granier, A., 2008. Impact of severe dry season on net ecosystem exchange in the Neotropical rainforest of French Guiana. *Global Change Biology* 14, 1917–1933.
- Borken, W., Savage, K., Davidson, E.A., Trumbore, S.E., 2006. Effects of experimental drought on soil respiration and radiocarbon efflux from a temperate forest soil. *Global Change Biology* 12, 177–193.
- Brieffa, K.R., Shishov, V.V., Melvin, T.M., Vaganov, E.A., Grudd, H., Hantemirov, R.M., Eronen, M., Naurzbaev, M.M., 2008. Trends in recent temperature and radial tree

- growth spanning 2000 years across northwest Eurasia. *Philosophical Transactions of the Royal Society B-Biological Sciences* 363, 2271–2284.
- Byrne, K.A., Kiely, G., Leahy, P., 2007. Carbon sequestration determined using farm scale carbon balance and eddy covariance. *Agricultural Ecosystems and Environment* 121, 357–364.
- Campbell, G.S., Norman, J.M., 1998. *An Introduction to Environmental Biophysics*. Springer-Verlag, New York.
- Carvalho, N., Reichstein, M., Ciais, P., Collatz, G.J., Mahecha, M.D., Montagnani, L., Papale, D., Rambal, S., Seixas, J., 2010. Identification of vegetation and soil carbon pools out of equilibrium in a process model via eddy covariance and biometric constraints. *Global Change Biology* 16, 2813–2829.
- Carvalho, N., Reichstein, M., Seixas, J., Collatz, G.J., Pereira, J.S., Berbigier, P., Carrara, A., Granier, A., Montagnani, L., Papale, D., Rambal, S., Sanz, M.J., Valentini, R., 2008. Implications of the carbon cycle steady state assumption for biogeochemical modeling performance and inverse parameter retrieval. *Global Biogeochemical Cycles* 22.
- Chester, D.L., 1990. Why two hidden layers are better than one. In: *Proceedings of the International Joint Conference on Neural Networks*, pp. 265–268.
- Chevallier, F., Chérut, F., Scott, N.A., Chédin, A., 1998. A neural network approach for a fast and accurate computation of a longwave radiative budget. *Journal of Applied Meteorology and Climatology* 37, 1385–1397.
- Cook, B.D., Davis, K.J., Wang, W.G., Desai, A., Berger, B.W., Teclaw, R.M., Martin, J.G., Bolstad, P.V., Bakwin, P.S., Yi, C.X., Heilman, W., 2004. Carbon exchange and venting anomalies in an upland deciduous forest in northern Wisconsin, USA. *Agricultural and Forest Meteorology* 126, 271–295.
- Crawford, T.M., Duchon, C.E., 1999. An improved parameterization for estimating effective atmospheric emissivity for use in calculating daytime downwelling longwave radiation. *Journal of Applied Meteorology* 38, 474–480.
- Dekker, S.C., Bouten, W., Schaap, M.G., 2001. Analysing forest transpiration model errors with artificial neural networks. *Journal of Hydrology* 246, 197–208.
- Desai, A.R., Bolstad, P.V., Cook, B.D., Davis, K.J., Carey, E.V., 2005. Comparing net ecosystem exchange of carbon dioxide between an old-growth and mature forest in the upper Midwest, USA. *Agricultural and Forest Meteorology* 128, 33–55.
- Dietze, M.C., Vargas, R., Richardson, A.D., Stoy, P.C., Barr, A.G., Anderson, R.S., Arain, M.A., Baker, I.T., Black, T.A., Chen, J.M., Ciais, P., Flanagan, L.B., Gough, C.M., Grant, R.F., Hollinger, D., Izaurralde, R.C., Kucharik, C.J., Laflaur, P., Liu, S., Lokupitiya, E., Luo, Y., Munger, J.W., Peng, C., Poulter, B., Price, D.T., Ricciuto, D.M., Riley, W.J., Sahoo, A.K., Schaefer, K., Suyker, A.E., Tian, H., Tonitto, C., Verbeek, H., Verma, S.B., Wang, W., Weng, E., 2011. Characterizing the performance of ecosystem models across time scales: a spectral analysis of the North American Carbon Program site-level synthesis. *Journal of Geophysical Research-Biogeosciences*, 116.
- Dolman, A.J., Moors, E.J., Elbers, J.A., 2002. The carbon uptake of a mid latitude pine forest growing on sandy soil. *Agricultural and Forest Meteorology* 111, 157–170.
- Don, A., Reibmann, C., Kolle, O., Scherer-lorenz, M., Schulze, E.D., 2009. Impact of afforestation-associated management changes on the carbon balance of grassland. *Global Change Biology* 15, 1990–2002.
- Dunn, A.L., Barford, C.C., Wofsy, S.C., Goulden, M.L., Daube, B.C., 2007. A long-term record of carbon exchange in a boreal black spruce forest: means, responses to interannual variability, and decadal trends. *Global Change Biology* 13, 577–590.
- Flanagan, L.B., Johnson, B.G., 2005. Interacting effects of temperature, soil moisture and plant biomass production on ecosystem respiration in a northern temperate grassland. *Agricultural and Forest Meteorology* 130, 237–253.
- Flanagan, L.B., Wever, L.A., Carlson, P.J., 2002. Seasonal and interannual variation in carbon dioxide exchange and carbon balance in a northern temperate grassland. *Global Change Biology* 8, 599–615.
- Foken, T., 2008. The energy balance closure problem: an overview. *Ecological Applications* 18, 1351–1367.
- Foken, T., Aubinet, M., Finnigan, J.J., Leclerc, M.Y., Mauder, M., Paw, U.K.T., 2011. Results of a panel discussion about the energy balance closure correction for trace gases. *Bulletin of the American Meteorological Society* 92, 13–18.
- Garbulska, M.F., Penuelas, J., Papale, D., Filella, I., 2008. Remote estimation of carbon dioxide uptake by a Mediterranean forest. *Global Change Biology* 14, 2860–2867.
- Ghil, M., Allen, M.R., Dettinger, M.D., Ide, K., Kondrashov, D., Mann, M.E., Robertson, A.W., Saunders, A., Tian, Y., Varadi, F., Yiou, P., 2002. Advanced spectral methods for climatic time series. *Reviews of Geophysics* 40, 1003.
- Gianelle, D., Vescovo, L., Marcolla, B., Manca, G., Cescatti, A., 2009. Ecosystem carbon fluxes and canopy spectral reflectance of a mountain meadow. *International Journal of Remote Sensing* 30, 435–449.
- Giasson, M.A., Coursolle, C., Margolis, H.A., 2006. Ecosystem-level CO₂ fluxes from a boreal cutover in eastern Canada before and after scarification. *Agricultural and Forest Meteorology* 140, 23–40.
- Gilmanov, T.G., Soussana, J.E., Aires, L., Allard, V., Ammann, C., Balzarolo, M., Barcza, Z., Bernhofer, C., Campbell, C.L., Cernusca, A., Cescatti, A., Clifton-Brown, J., Dirks, B.O.M., Dore, S., Eugster, W., Fuhrer, J., Gimeno, C., Gruenwald, T., Haszpra, L., Hensen, A., Ibrom, A., Jacobs, A.F.G., Jones, M.B., Lanigan, G., Laurila, T., Lohila, A., Manca, G., Marcolla, B., Nagy, Z., Pilegaard, K., Pinter, K., Pio, C., Raschi, A., Rogiers, N., Sanz, M.J., Stefani, P., Sutton, M., Tuba, Z., Valentini, R., Williams, M.L., Wohlfahrt, G., 2007. Partitioning European grassland net ecosystem CO₂ exchange into gross primary productivity and ecosystem respiration using light response function analysis. *Agriculture Ecosystems & Environment* 121, 93–120.
- Gilmanov, T.G., Tieszen, L.L., Wylie, B.K., Flanagan, L.B., Frank, A.B., Haferkamp, M.R., Meyers, T.P., Morgan, J.A., 2005. Integration of CO₂ flux and remotely-sensed data for primary production and ecosystem respiration analyses in the Northern Great Plains: potential for quantitative spatial extrapolation. *Global Ecology and Biogeography* 14, 271–292.
- Göckede, M., Turner, D.P., Michalak, A.M., Vickers, D., Law, B.E., 2010. Sensitivity of a sub-regional scale atmospheric inverse CO₂ modeling framework to boundary conditions. *Journal of Geophysical Research* 115, D24112, <http://dx.doi.org/10.1029/2010JD014443>.
- Golyandina, N., Nekrutkin, V., Zhigljavsky, A., 2001. *Analysis of Time Series Structure: SSA and Related Techniques*. Monographs on Statistics and Applied Probability No. 90. Chapman & Hall/CRC, Boca Raton.
- Gough, C.M., Vogel, C.S., Schmid, H.P., Su, H.B., Curtis, P.S., 2008. Multi-year convergence of biometric and meteorological estimates of forest carbon storage. *Agricultural and Forest Meteorology* 148, 158–170.
- Goulden, M.L., Munger, J.W., Fan, S.M., Daube, B.C., Wofsy, S.C., 1996. Measurements of carbon sequestration by long-term eddy covariance: methods and a critical evaluation of accuracy. *Global Change Biology* 2, 169–182.
- Granier, A., Ceschia, E., Damesin, C., Duffrene, E., Epron, D., Gross, P., Lebaube, S., Le Dantec, V., Le Goff, N., Lemoine, D., Lucot, E., Ottorini, J.M., Pontailler, J.Y., Saugier, B., 2000. The carbon balance of a young Beech forest. *Functional Ecology* 14, 312–325.
- Grunwald, T., Bernhofer, C., 2007. A decade of carbon, water and energy flux measurements of an old spruce forest at the Anchor Station Tharandt. *Tellus Series B-Chemical and Physical Meteorology* 59, 387–396.
- Hollinger, D.Y., Aber, J., Dail, B., Davidson, E.A., Goltz, S.M., Hughes, H., Leclerc, M.Y., Lee, J.T., Richardson, A.D., Rodrigues, C., Scott, N.A., Achuatavariar, D., Walsh, J., 2004. Spatial and temporal variability in forest-atmosphere CO₂ exchange. *Global Change Biology* 10, 1689–1706.
- Hollinger, D.Y., Goltz, S.M., Davidson, E.A., Lee, J.T., Tu, K., Valentine, H.T., 1999. Seasonal patterns and environmental control of carbon dioxide and water vapour exchange in an ecton boreal forest. *Global Change Biology* 5, 891–902.
- Hollinger, D.Y., Richardson, A.D., 2005. Uncertainty in eddy covariance measurements and its application to physiological models. *Tree Physiology* 25, 873–885.
- Hudiburg, T., Law, B.E., Turner, D.P., Campbell, J., Donato, D., Duane, M., 2009. Carbon dynamics of Oregon and Northern California forests and potential land-based carbon storage. *Ecological Applications* 19, 163–180.
- Hui, D.F., Luo, Y.Q., Katul, G., 2003. Partitioning interannual variability in net ecosystem exchange between climatic variability and functional change. *Tree Physiology* 23, 433–442.
- Humphreys, E.R., Black, T.A., Morgenstern, K., Cai, T.B., Drewitt, G.B., Nescic, Z., Trofymow, J.A., 2006. Carbon dioxide fluxes in coastal Douglas-fir stands at different stages of development after clearcut harvesting. *Agricultural and Forest Meteorology* 140, 6–22.
- Jaksic, V., Kiely, G., Albertson, J., Oren, R., Katul, G., Leahy, P., Byrne, K., 2006. Net ecosystem exchange of grassland in contrasting wet and dry years. *Agricultural and Forest Meteorology* 139, 323–334.
- Jung, M., Reichstein, M., Margolis, H.A., Cescatti, A., Richardson, A.D., Arain, M.A., Arneth, A., Bernhofer, C., Bonal, D., Chen, J., Gianelle, D., Gobron, N., Kiely, G., Kutsch, W., Lasslop, G., Law, B.E., Lindroth, A., Merbold, L., Montagnani, L., Moors, E.J., Papale, D., Sottocornola, M., Vaccari, F., Williams, C., 2011. Global patterns of land-atmosphere fluxes of carbon dioxide, latent heat, and sensible heat derived from eddy covariance, satellite, and meteorological observations. *Journal of Geophysical Research-Biogeosciences* 116.
- Katul, G., Lai, C.T., Schafer, K., Vidakovic, B., Albertson, J., Ellsworth, D., Oren, R., 2001. Multiscale analysis of vegetation surface fluxes: from seconds to years. *Advances in Water Resources* 24, 1119–1132.
- Keenan, T.F., Baker, I., Barr, A., Ciais, P., Davis, K., Dietze, M., Dragon, D., Gough, C.M., Grant, R., Hollinger, D., Hufkens, K., Poulter, B., McCaughey, H., Raczka, B., Ryu, Y., Schaefer, K., Tian, H., Verbeek, H., Zhao, M., Richardson, A.D., 2012a. Terrestrial biosphere model performance for inter-annual variability of land-atmosphere CO₂ exchange. *Global Change Biology* 18, 1971–1987.
- Keenan, T.F., Davidson, E., Moffat, A.M., Munger, W., Richardson, A.D., 2012b. Using model-data fusion to interpret past trends, and quantify uncertainties in future projections, of terrestrial ecosystem carbon cycling. *Global Change Biology*, <http://dx.doi.org/10.1111/j.1365-2486.2012.02684.x>.
- Kljun, N., Black, T.A., Griffis, T.J., Barr, A.G., Gaumont-Guay, D., Morgenstern, K., McCaughey, J.H., Nescic, Z., 2006. Response of net ecosystem productivity of three boreal forest stands to drought. *Ecosystems* 9, 1128–1144.
- Knohl, A., Schulze, E.D., Kolle, O., Buchmann, N., 2003. Large carbon uptake by an unmanaged 250-year-old deciduous forest in Central Germany. *Agricultural and Forest Meteorology* 118, 151–167.
- Kondrashov, D., Ghil, M., 2006. Spatio-temporal filling of missing points in geophysical data sets. *Nonlinear Processes in Geophysics* 13, 151–159.
- Krinner, G., Viovy, N., de Noblet-Ducoudre, N., Ogee, J., Polcher, J., Friedlingstein, P., Ciais, P., Sitch, S., Prentice, I.C., 2005. A dynamic global vegetation model for studies of the coupled atmosphere-biosphere system. *Global Biogeochemical Cycles* 19.
- Kutsch, W.L., Aubinet, M., Buchmann, N., Smith, P., Osborne, B., Eugster, W., Wattenbach, M., Schurmpf, M., Schulze, E.D., Tomelleri, E., Ceschia, E., Bernhofer, C., Beziat, P., Carrara, A., Di Tommasi, P., Gruenwald, T., Jones, M., Magliulo, V., Marloie, O., Moureaux, C., Oliosio, A., Sanz, M.J., Saunders, M., Sogaard, H., Ziegler, W., 2010b. The net biome production of full crop rotations in Europe. *Agriculture Ecosystems & Environment* 139, 336–345.
- Kutsch, W.L., Persson, T., Schurmpf, M., Moyano, F.E., Mund, M., Andersson, S., Schulze, E.-D., 2010a. Heterotrophic soil respiration and soil carbon dynamics in the deciduous Hainich forest obtained by three approaches. *Biogeochemistry* 100, 167–183.
- Lasslop, G., Reichstein, M., Kattge, J., Papale, D., 2008. Influences of observation errors in eddy flux data on inverse model parameter estimation. *Biogeosciences* 5, 1311–1324.

- Law, B.E., Thornton, P.E., Irvine, J., Anthoni, P.M., Van Tuyl, S., 2001. Carbon storage and fluxes in ponderosa pine forests at different developmental stages. *Global Change Biology* 7, 755–777.
- Le Maire, G., Delpierre, N., Jung, M., Ciais, P., Reichstein, M., Viovy, N., Granier, A., Ibrom, A., Kolari, P., Longdoz, B., Moors, E.J., Pilegaard, K., Rambal, S., Richardson, A.D., Vesala, T., 2010. Detecting the critical periods that underpin interannual fluctuations in the carbon balance of European forests. *Journal of Geophysical Research-Biogeosciences* 115.
- Li, L., Vuichard, N., Viovy, N., Ciais, P., Wang, T., Ceschia, E., Jans, W., Wattenbach, M., Béziat, P., Gruenwald, T., Lehuger, S., Bernhofer, C., 2011. Importance of crop varieties and management practices: evaluation of a process-based model for simulating CO₂ and H₂O fluxes at five European maize (*Zea mays* L.) sites. *Biogeosciences* 8, 1721–1736.
- Leuning, R., van Gorsel, E., Massman, W.J., Isaac, P.R., 2012. Reflections on the surface energy imbalance problem. *Agricultural and Forest Meteorology* 156, 65–74.
- Ma, S., Baldocchi, D.D., Xu, L., Hehn, T., 2007. Inter-annual variability in carbon dioxide exchange of an oak/grass savanna and open grassland in California. *Agricultural and Forest Meteorology* 147, 157–171.
- Mahecha, M.D., Reichstein, M., Carvalhais, N., Lasslop, G., Lange, H., Seneviratne, S.I., Vargas, R., Ammann, C., Arain, M.A., Cescatti, A., Janssens, I.A., Migliavacca, M., Montagnani, L., Richardson, A.D., 2010b. Global convergence in the temperature sensitivity of respiration at ecosystem level. *Science* 329, 838–840.
- Mahecha, M.D., Reichstein, M., Jung, M., Seneviratne, S.I., Zaehle, S., Beer, C., Braakhekke, M.C., Carvalhais, N., Lange, H., Le Maire, G., Moors, E., 2010a. Comparing observations and process-based simulations of biosphere-atmosphere exchanges on multiple timescales. *Journal of Geophysical Research-Biogeosciences* 115.
- Mahecha, M.D., Reichstein, M., Lange, H., Carvalhais, N., Bernhofer, C., Gruenwald, T., Papale, D., Seufert, G., 2007. Characterizing ecosystem-atmosphere interactions from short to interannual time scales. *Biogeosciences* 4, 743–758.
- Marchesini, L.B., Papale, D., Reichstein, M., Vuichard, N., Tchekakova, N., Valentini, R., 2007. Carbon balance assessment of a natural steppe of southern Siberia by multiple constraint approach. *Biogeosciences* 4, 581–595.
- Marcolla, B., Cescatti, A., 2005. Experimental analysis of flux footprint for varying stability conditions in an alpine meadow. *Agricultural and Forest Meteorology* 135, 291–301.
- Mellesse, A.M., Hanley, R.S., 2005. Artificial neural network application for multi-ecosystem carbon flux simulation. *Ecological Modelling* 189, 305–314.
- Merbold, L., Kutsch, W.L., Corradi, C., Kolle, O., Rebmann, C., Stoy, P.C., Zimov, S.A., Schulze, E.D., 2009. Artificial drainage and associated carbon fluxes (CO₂/CH₄) in a tundra ecosystem. *Global Change Biology* 15, 2599–2614.
- Meyers, T.P., Hollinger, S.E., 2004. An assessment of storage terms in the surface energy balance of maize and soybean. *Agricultural and Forest Meteorology* 125, 105–115.
- McCaughey, J.H., Pejam, M.R., Arain, M.A., Cameron, D.A., 2006. Carbon dioxide and energy fluxes from a boreal mixedwood forest ecosystem in Ontario. *Canadian Society of Agriculture and Forest Meteorology* 140, 79–96.
- Migliavacca, M., Meroni, M., Manca, G., Matteucci, G., Montagnani, L., Grassi, G., Zenone, T., Teobaldelli, M., Godeed, L., Colombo, R., Seufert, G., 2009. Seasonal and interannual patterns of carbon and water fluxes of a poplar plantation under peculiar eco-climatic conditions. *Agricultural and Forest Meteorology* 149, 1460–1476.
- Milyukova, I.M., Kolle, O., Varlagin, A.V., Vygodskaya, N.N., Schulze, E.D., Lloyd, J., 2002. Carbon balance of a southern taiga spruce stand in European Russia. *Tellus Series B-Chemical and Physical Meteorology* 54, 429–442.
- Mkhabela, M.S., Amiro, B.D., Barr, A.G., Black, T.A., Hawthorne, I., Kidston, J., McCaughey, J.H., Orchanisky, A.L., Nescic, Z., Sass, A., Shashkov, A., Zha, T., 2009. Comparison of carbon dynamics and water use efficiency following fire and harvesting in Canadian boreal forests. *Agricultural and Forest Meteorology* 149, 783–794.
- Moffat, A.M., Beckstein, C., Churkina, G., Mund, M., Heimann, M., 2010. Characterization of ecosystem responses to climatic controls using artificial neural networks. *Global Change Bi* 16, 2737–2749.
- Montagnani, L., Manca, G., Canepa, E., Georgieva, E., Acosta, M., Feigenwinter, C., Janous, D., Kerschbaumer, G., Lindroth, A., Minach, L., Minerbi, S., Molder, M., Pavelka, M., Seufert, G., Zeri, M., Ziegler, W., 2009. A new mass conservation approach to the study of CO₂ advection in an alpine forest. *Journal of Geophysical Research-Atmospheres* 114.
- Morshed, J., Kaluarachchi, J.J., 1998. Application of artificial neural network and genetic algorithm in flow and transport simulations. *Advances in Water Resources* 22, 145–158.
- Nicks, A.D., Williams, J.R., Richardson, C.W., Lane, L.J., 1987. Generating Climatic Data for a Water Erosion Prediction Model. ASAE, Paper No. 87-2541, St. Joseph, MI.
- Papale, D., Reichstein, M., Aubinet, M., Canfora, E., Bernhofer, C., Kutsch, W., Longdoz, B., Rambal, S., Valentini, R., Vesala, T., Yakir, D., 2006. Towards a standardized processing of Net Ecosystem Exchange measured with eddy covariance technique: algorithms and uncertainty estimation. *Biogeosciences* 3, 571–583.
- Peichl, M., Leava, N.A., Kiely, G., 2011. Above- and belowground ecosystem biomass, carbon and nitrogen allocation in recently afforested grassland and adjacent intensively managed grassland. *Plant and Soil*, 1–16.
- Peichl, M., Arain, M.A., 2007. Allometry and partitioning of above- and belowground tree biomass in an age-sequence of white pine forests. *Forest Ecology and Management* 253, 68–80.
- Pejam, M.R., Arain, M.A., McCaughey, J.H., 2006. Energy and water vapour exchanges over a mixedwood forest in Ontario, Canada. *Hydrological Processes* 20, 3709–3724.
- Pietsch, S.A., Hasenauer, H., 2006. Evaluating the self-initialization procedure for large-scale ecosystem models. *Global Change Biology* 12, 1658–1669.
- Pilegaard, K., Mikkelsen, T.N., Beier, C., Jensen, N.O., Ambus, P., Ro-Poulsen, H., 2003. Field measurements of atmosphere-biosphere interactions in a Danish beech forest. *Boreal Environment Research* 8, 315–333.
- Rebmann, C., Zeri, M., Lasslop, G., Mund, M., Kolle, O., Schulze, E.-D., Feigenwinter, C., 2010. Treatment and assessment of the CO₂-exchange at a complex forest site in Thuringia, Germany. *Agricultural and Forest Meteorology* 150, 684–691.
- Reichstein, M., Falge, E., Baldocchi, D., Papale, D., Aubinet, M., Berbigier, P., Bernhofer, C., Buchmann, N., Gilmanov, T., Granier, A., Grunwald, T., Havrankova, K., Ilvesniemi, H., Janous, D., Knohl, A., Laurila, T., Lohila, A., Loustau, D., Matteucci, G., Meyers, T., Miglietta, F., Ourcival, J.M., Pumpanen, J., Rambal, S., Rotenberg, E., Sanz, M., Tenhunen, J., Seufert, G., Vaccari, F., Vesala, T., Yakir, D., Valentini, R., 2005. On the separation of net ecosystem exchange into assimilation and ecosystem respiration: review and improved algorithm. *Global Change Biology* 11, 1424–1439.
- Rey, A., Pegoraro, E., Tedeschi, V., De Parri, I., Jarvis, P.G., Valentini, R., 2002. Annual variation in soil respiration and its components in a coppice oak forest in Central Italy. *Global Change Biology* 8, 851–866.
- Ricciotto, D.M., Butler, M.P., Davis, K.J., Cook, B.D., Bakwin, P.S., Andrews, A., Teclaw, R.M., 2008. Causes of interannual variability in ecosystem-atmosphere CO₂ exchange in a northern Wisconsin forest using a Bayesian model calibration. *Agricultural and Forest Meteorology* 148, 309–327.
- Richardson, A.D., Hollinger, D.Y., Aber, J.D., Ollinger, S.V., Braswell, B.H., 2007. Environmental variation is directly responsible for short- but not long-term variation in forest-atmosphere carbon exchange. *Global Change Biology* 13, 788–803.
- Richardson, A.D., Mahecha, M.D., Falge, E., Kattge, J., Moffat, A.M., Papale, D., Reichstein, M., Stauch, V.J., Braswell, B.H., Churkina, G., Kruijt, B., Hollinger, D.Y., 2008. Statistical properties of random CO₂ flux measurement uncertainty inferred from model residuals. *Agricultural and Forest Meteorology* 148, 38–50.
- Richardson, A.D., Anderson, R.S., Arain, M.A., Barr, A.G., Bohrer, G., Chen, G., Chen, J.M., Ciais, P., Davis, K.J., Desai, A.R., Dietze, M.C., Dragoni, D., Garrity, S.R., Gough, C.M., Grant, R., Hollinger, D.Y., Margolis, H.A., McCaughey, H., Migliavacca, M., Monson, R.K., Mungler, J.W., Poulter, B., Raczka, B.M., Ricciotto, D.M., Sahoo, A.K., Schaefer, K., Tian, H., Vargas, R., Verbeek, H., Xiao, J., Xue, Y., 2012. Terrestrial biosphere models need better representation of vegetation phenology: results from the North American Carbon Program Site Synthesis. *Global Change Biology* 18, 566–584.
- Rumelhart, D.E., Hinton, G.E., Williams, R.J., 1986. Learning internal representations by error propagation. In: Rumelhart, D.E., McClelland, J.L., the, P.D.P., Research Group (Eds.), *Paralleled Distributed Processing. Explorations in the Microstructure of Cognition. Volume 1: Foundations*. The MIT Press, Cambridge, MA, pp. 318–362.
- Scardi, M., 2001. Advances in neural network modeling of phytoplankton primary production. *Ecological Modeling* 146, 33–45.
- Schaefer, K., Schwalm, C., Williams, C., Arain, M.A., Barr, A., Chen, J., Davis, K.J., Dimitrovs, D., Hilton, T.W., Hollinger, D.Y., Humphreys, E., Poulter, B., Raczka, B.M., Richardson, A.D., Sahoo, A., Thornton, P., Vargas, R., Verbeek, H., Anderson, R., Baker, I., Black, T.A., Bolstad, P., Chen, J., Curtis, P., Desai, A.R., Dietze, M., Dragoni, D., Gough, C., Grant, R.F., Gu, L., Jain, A., Kucharik, C., Law, B.E., Liu, S., Lokipitiya, E., Margolis, H.A., Matamala, R., McCaughey, J.H., Monson, R., Mungler, J.W., Oechel, W., Peng, C., Price, D.T., Ricciotto, D., Riley, W.J., Roulet, N., Tian, H., Tonitto, C., Torn, M., Weng, E., Zhou, X., 2012. A model-data comparison of gross primary productivity: results from the North American carbon program site synthesis. *Journal of Geophysical Research* 117, G03010, <http://dx.doi.org/10.1029/2012JG001960>.
- Schimel, D., Churkina, G., Braswell, B.H., Trenbath, J., 2005. Remembrance of weather past: ecosystem responses to climate variability. *History of atmospheric CO₂ and its effects on plants. Animals, and Ecosystems* 177, 350–368.
- Schmid, H.P., Grimmond, C.S.B., Cropley, F., Offerle, B., Su, H.B., 2000. Measurements of CO₂ and energy fluxes over a mixed hardwood forest in the mid-western United States. *Agricultural and Forest Meteorology* 103, 357–374.
- Schwalm, C., Williams, C., Schaeffer, K., Anderson, R., Arain, M.A., Baker, I., Barr, A., Black, A., Chen, G., Chen, J., Ciais, P., Davis, K.J., Desai, A., Dietze, M., Dragoni, D., Fischer, M., Flanagan, L., Grant, R., Gu, L., Hollinger, D., Izaurredd, R.C., Kucharik, C., LaFleur, P., Law, B.E., Li, L., Li, Z., Liu, S., Luo, Y., Ma, S., Margolis, A., Matamala, R., McCaughey, H., Monson, R.K., Oechel, W.C., Peng, C., Poulter, B., Price, D.T., Ricciotto, D.M., Riley, W., Sahoo, A.K., Sprintsin, M., Sun, J., Tian, H., Tonitto, C., Verbeek, H., Verma, S., 2010. A model-data intercomparison of CO₂ exchange across North America: results from the North American carbon program site synthesis. *Journal of Geophysical Research* 115, G00H05, <http://dx.doi.org/10.1029/2009JG001229>.
- Sierra, C.A., Loescher, H.W., Harmon, M.E., Richardson, A.D., Hollinger, D.Y., Perakis, S.S., 2009. Interannual variation of carbon fluxes from three contrasting evergreen forests: the role of forest dynamics and climate. *Ecology* 90, 2711–2723.
- Siqueira, M.B., Katul, G.G., Sampson, D.A., Stoy, P.C., Juang, J.Y., McCarthy, H.R., Oren, R., 2006. Multiscale model intercomparisons of CO₂ and H₂O exchange rates in a maturing southeastern US pine forest. *Global Change Biology* 12, 1189–1207.
- Smith, P.C., De Noblet-Ducoudre, N., Ciais, P., Peylin, P., Viovy, N., Meurdesoif, Y., Bondeau, A., 2010. European-wide simulations of croplands using an improved terrestrial biosphere model: phenology and productivity. *Journal of Geophysical Research-Biogeosciences* 115.
- Staudt, K., Foken, T., 2007. Documentation of reference data for the experimental areas of the Bayreuth Centre for Ecology and Environmental Research (BayCEER)

- at the Waldstein site. *Arbeitsergebn, Univ Bayreuth, Abt Mikrometeorol* ISSN 1614-8916, p. 35.
- Stoy, P.C., Richardson, A.D., Baldocchi, D.D., Katul, G.G., Stanovick, J., Mahecha, M.D., Reichstein, M., Detto, M., Law, B.E., Wohlfahrt, G., Arriga, N., Campos, J., McCaughey, J.H., Montagnani, L., Paw, U., Sevanto, K.T., Williams, S.M., 2009. Biosphere-atmosphere exchange of CO₂ in relation to climate: a cross-biome analysis across multiple time scales. *Biogeosciences* 6, 2297–2312.
- Suni, T., Berninger, F., Markkanen, T., Keronen, P., Rannik, U., Vesala, T., 2003a. Inter-annual variability and timing of growing-season CO₂ exchange in a boreal forest. *Journal of Geophysical Research-Atmospheres*, 108.
- Suni, T., Rinne, J., Reissell, A., Altimir, N., Keronen, P., Rannik, U., Dal Maso, M., Kulmala, M., Vesala, T., 2003b. Long-term measurements of surface fluxes above a Scots pine forest in Hyttiala, southern Finland, 1996–2001. *Boreal Environment Research* 8, 287–301.
- Tedeschi, V., Rey, A., Manca, G., Valentini, R., Jarvis, P.G., Borghetti, M., 2006. Soil respiration in a Mediterranean oak forest at different developmental stages after coppicing. *Global Change Biology* 12, 110–121.
- Thomas, C.K., Law, B.E., Irvine, J., Martin, J.G., Pettijohn, J.C., Davis, K.J., 2009. Seasonal hydrology explains interannual and seasonal variation in carbon and water exchange in a semi-arid mature ponderosa pine forest in central Oregon. *Journal of Geophysical Research* 114, G04006, <http://dx.doi.org/10.1029/2009JG001010>.
- Thomas, V., Noland, T., Treitz, P., McCaughey, J.H., 2011. Leaf area and clumping indices for a boreal mixed-wood forest: lidar, hyperspectral, and Landsat models. *International Journal of Remote Sensing* 32 (23), 8271–8297.
- Thornton, P., Law, B.E., Gholz, H., Clark, K.L., Falge, E., Ellsworth, D.H., Goldstein, A.H., Monson, R.K., Hollinger, D., Falk, M., Chen, J., Sparks, J.P., 2002. Modeling and measuring the effects of disturbance history and climate on carbon and water budgets in evergreen needleleaf forests. *Agricultural and Forest Meteorology* 113, 185–222.
- Thum, T., Aaloto, T., Laurila, T., Aurela, M., Hatakka, J., Lindroth, A., Vesala, T., 2009. Spring initiation and autumn cessation of boreal coniferous forest CO₂ exchange assessed by meteorological and biological variables. *Tellus* 61B, 701–717.
- Urbanski, S., Barford, C., Wofsy, S., Kucharik, C., Pyle, E., Budney, J., McKain, K., Fitzjarrald, D., Czirkowsky, M., Munger, J.W., 2007. Factors controlling CO₂ exchange on timescales from hourly to decadal at Harvard Forest. *Journal of Geophysical Research-Biogeosciences* 112.
- van der Molen, M.K., Dolman, A.J., Ciais, P., Eglin, T., Gobron, N., Law, B.E., Meir, P., Peters, W., Phillips, O.L., Reichstein, M., Chen, T., Dekker, S.C., Doubkova, M., Friedl, M.A., Jung, M., van den Hurk, B.J.J.M., de Jeu, R.A.M., Kruijt, B., Ohta, T., Rebel, K.T., Plummer, S., Seneviratne, S.I., Sitch, S., Teuling, A.J., van der Werf, G.R., Wang, G., 2011. Drought and ecosystem carbon cycling. *Agricultural and Forest Meteorology* 151, 765–773.
- van Wijk, M.T., Bouten, W., 1999. Water and carbon fluxes above European coniferous forests modelled with artificial neural networks. *Ecological Modelling* 120, 181–197.
- Verma, S.B., Dobermann, A., Cassman, K.G., Walters, D.T., Knops, J.M., Arkebauer, T.J., Suyker, A.E., Burba, G.G., Amos, B., Yang, H.S., Ginting, D., Hubbard, K.G., Gitelson, A.A., Walter-Shea, E.A., 2005. Annual carbon dioxide exchange in irrigated and rainfed maize-based agroecosystems. *Agricultural and Forest Meteorology* 131, 77–96.
- Vickers, D., Gockede, M., Law, B.E., 2010. Uncertainty estimates for 1-hour averaged turbulence fluxes of carbon dioxide, latent heat and sensible heat. *Tellus B* 62, 87–99.
- Vickers, D., Thomas, C., Law, B.E., 2009. Random and systematic CO₂ flux sampling errors for tower measurements over forests in the convective boundary layer. *Agricultural and Forest Meteorology* 149, 73–83.
- Wang, X., Piao, S., Ciais, P., Janssens, I.A., Reichstein, M., Peng, S., Wang, T., 2010. Are ecological gradients in seasonal Q(10) of soil respiration explained by climate or by vegetation seasonality? *Soil Biology & Biochemistry* 42, 1728–1734.
- Wang, Y.P., Kowalczyk, E., Leuning, R., Abramowitz, G., Raupach, M.R., Pak, B., van Gorsel, E., Luhar, A., 2011. Diagnosing errors in a land surface model (CABLE) in the time and frequency domains. *Journal of Geophysical Research-Biogeosciences* 116.
- Williams, M., Richardson, A.D., Reichstein, M., Stoy, P.C., Peylin, P., Verbeeck, H., Carvalhais, N., Jung, M., Hollinger, D.Y., Kattge, J., Leuning, R., Luo, Y., Tomelleri, E., Trudinger, C.M., Wang, Y.P., 2009. Improving land surface models with FLUXNET data. *Biogeosciences* 6, 1341–1359.
- Wilson, K., Goldstein, A., Falge, E., Aubinet, M., Baldocchi, D., Bernhofer, P., Bernhofer, C., Ceulemans, R., Dolman, H., Field, C., Grelle, A., Ibrom, A., Law, B.E., Kowalski, A., Meyers, T., Moncrieff, J., Monson, R., Oechel, W., Tenhunen, J., Valentini, R., Verma, S., 2002. Energy balance closure at FLUXNET sites. *Agricultural and Forest Meteorology* 113, 223–243.
- Wohlfahrt, G., Anderson-Dunn, M., Bahn, M., Balzarolo, M., Berninger, F., Campbell, C., Carrara, A., Cescatti, A., Christensen, T., Dore, S., Eugster, W., Friborg, T., Furger, M., Gianelle, D., Gimeno, C., Hargreaves, K., Hari, P., Haslwanter, A., Johansson, T., Marcolla, B., Milford, C., Nagy, Z., Nemitz, E., Rogiers, N., Sanz, M.J., Siegwolf, R.T.W., Susiluoto, S., Sutton, M., Tuba, Z., Ugolini, F., Valentini, R., Zorer, R., Cernusca, A., 2008. Biotic, abiotic, and management controls on the net ecosystem CO₂ exchange of European mountain grassland ecosystems. *Ecosystems* 11, 1338–1351.
- Wutzler, T., Reichstein, M., 2007. Soils apart from equilibrium—consequences for soil carbon balance modelling. *Biogeosciences* 4, 125–136.
- Yiou, P., Sornette, D., Ghil, M., 2000. Data-adaptive wavelets and multi-scale singular-spectrum analysis. *Physica D: Nonlinear Phenomena* 142, 254–290.
- Zhang, G., Eddy Patuwo, B., Hu, M.Y., 1998. Forecasting with artificial neural networks: the state of the art. *International journal of forecasting* 14 (1), 35–62.
- Zreda, M., Shuttleworth, W.J., Zeng, X., Zweck, C., Desilets, D., Franz, T., Rosolem, R., Ferre, T.P.A., 2012. COSMOS: the COSmic-ray Soil Moisture Observing System. *Hydrology and Earth System Science Discussions* 9 (4), 4505–4551.